NASA Contractor Report 189637
ICASE Report No. 92–15

ICASE

ON THE STABILITY OF NONLINEAR VISCOUS VORTICES IN THREE-DIMENSIONAL BOUNDARY LAYERS

Andrew P. Bassom
S. R. Otto

Contract No. NAS1–18605
April 1992

Institute for Computer Applications in Science and Engineering
NASA Langley Research Center
Hampton, Virginia 23665–5225

Operated by the Universities Space Research Association

National Aeronautics and
Space Administration

Langley Research Center
Hampton, Virginia 23665-5225

ON THE STABILITY OF NONLINEAR VISCOUS VORTICES IN THREE–DIMENSIONAL BOUNDARY LAYERS

Andrew P. Bassom
Department of Mathematics
University of Exeter, North Park Road
Exeter, Devon. EX4 4QE, UK

S. R. Otto*
ICASE, Mailstop 132c
NASA Langley Research Center
Hampton, VA 23665–5225, USA

Abstract

Recently it has been demonstrated that three–dimensionality can play an important role in dictating the stability properties of any Görtler vortices which a particular boundary layer may support. According to a linearised theory vortices within a high Görtler number flow can take one of two possible forms within a two–dimensional flow supplemented by a small crossflow of size $O(R_\epsilon^{-\frac{1}{2}} G^{\frac{3}{5}})$ where R_ϵ is the Reynolds number of the flow and G the Görtler number. Bassom & Hall (1991) showed that these forms are characterised by O(1) wavenumber inviscid disturbances and larger, $O(G^{\frac{1}{5}})$, wavenumber modes which are trapped within a thin layer adjacent to the bounding surface. Here we concentrate on the latter, essentially viscous vortices and describe their weakly nonlinear stability properties in the presence of crossflow. It is shown conclusively that the effect of crossflow is to stabilise the nonlinear disturbances and the calculations herein allow stable, finite amplitude perturbations to be found. Predictions are made concerning the likelihood of observing some of these viscous modes within a practical setting and asymptotic work permits discussion of the stability properties of modes with wavenumbers which are small relative to the implied $O(G^{\frac{1}{5}})$ scaling.

* Research was supported by the National Aeronautics and Space Administration under NASA contract No. NAS1–18605 while the author was in residence at the Institute for Computer Applications in Science and Engineering (ICASE), NASA Langley Research Center, Hampton, VA 23665

§1 Introduction

Recently there has been interest in the effect of boundary layer growth on instability mechanisms to which the boundary layers are susceptible. Here concentration is focussed on the Görtler vortex mechanism which has been shown to occur in both two- and three- dimensional boundary layer flows over concave walls. Much of the early theoretical work concerned with Görtler vortices addressed the problem of describing the linear stability of external two-dimensional flows over such boundaries. Early contributions were made by, among others, Görtler (1940), Smith (1955) and Hämmerlin (1956). Later Hall (1982a,b) argued that much of this early work is fundamentally flawed for all the analyses invoked the parallel flow approximation (which essentially assumes that the basic flow in which the vortices lie is independent of the streamwise co-ordinate and so neglects the effect of boundary layer growth). This approximation enables the linear stability equations to be expressed as ordinary differential equations but Hall illustrated that this assumption is unjustifiable except in the limit of a small vortex wavelength, and indeed this is the explanation for the considerable inconsistencies in the results of the previous studies (see the review article Hall (1990) for fuller details). Additionally, in the case of a small vortex wavelength the Görtler instability may be described by an asymptotic structure which takes account of boundary layer growth in a rational manner and thence the parallel flow assumption is rendered unnecessary in the one situation in which it has any relevance.

Hall (1982a) examined boundary layer flow over the cylinder $y = 0$, $-\infty < z < \infty$ where the z-axis is a generator of the cylinder and y measures the distance normal to the surface. The x- co-ordinate measures distance along the curved surface, which is taken to have variable curvature

$$(1/b)\chi\,(x/l)\,, \tag{1.1a}$$

where b is a typical radius of curvature of the surface and l is a characteristic lengthscale in the streamwise direction. The Reynolds number R_e, the curvature parameter δ and the Görtler number G are defined by

$$R_e = U_0 l/\nu, \qquad \delta = l/b, \qquad G = 2R_e^{\frac{1}{2}}\delta, \tag{1.1b}$$

where U_0 is a typical flow velocity in the x direction and ν is the kinematic viscosity of the fluid. Hall (1982a) investigated the flow characteristics when R_e is large and δ is small such that in the limit $\delta \longrightarrow 0$, G is held fixed at an O(1) value. By scaling the

spanwise co-ordinate z on the boundary layer thickness, it was demonstrated that for a non-dimensional vortex wavenumber $\varepsilon^{-1} \gg 1$, linearised vortex modes within a two-dimensional basic flow are neutrally stable at a Görtler number $G = g_0\varepsilon^{-4} + \ldots$, where g_0 is a known O(1) constant whose precise value is dependent upon the properties of the underlying basic flow. For larger wavelengths the problem is fully nonparallel and the linear stability equations, which now take the form of a set of partial differential equations, have to be solved numerically, see Hall (1983). This paper showed two significant features of this nonparallel flow problem, namely that the ideas of a unique stability curve and of unique growth rates at a specified downstream location are inapplicable to the Görtler problem because the location where a vortex commences to grow is dependent upon the position and the shape of the imposed disturbance.

Hall (1988) addressed questions concerning the development of nonlinear nonparallel vortices within boundary layers. This numerical investigation showed that as the nonlinear disturbance evolves the perturbation energy becomes concentrated in the fundamental and mean flow correction; a conclusion consistent with the weakly nonlinear theory of Hall (1982b) valid for small wavelength vortices. It is well known that Görtler vortices set up by experimental means conserve their wavelength as they move downstream. Since the boundary layer itself thickens it follows that the local nondimensional vortex wavenumber becomes large as the vortex develops. Thus the small wavelength limit in the external Görtler problem is appropriate to the ultimate development of any fixed wavelength vortex and hence sufficiently far downstream in many flows the asymptotic work of Hall (1982a,b) becomes applicable.

As with all weakly nonlinear investigations the results of Hall (1982b) are valid only within a neighbourhood of the point where the imposed perturbation is neutrally stable. For vortices of wavenumber $\varepsilon^{-1} \gg 1$, their development downstream of the point of neutral stability is governed by the solution of a pair of coupled nonlinear partial differential equations which adopt a simple asymptotic structure at large values of X, where εX ($X = O(1)$) denotes the distance of the vortex downstream of the neutral point. Formally, for large X, Hall & Lakin (1988) showed that this asymptotic structure could be used to deduce the flow configuration for fully nonlinear Görtler vortices, at which point the mean flow correction generated by the presence of the vortices is as large as the basic (undisturbed) flow itself. The vortex structure derived by Hall & Lakin essentially consists of a core region in which the vortex is concentrated and which is bounded by two thin layers in which the vortex activity is reduced to zero exponentially. Further work by Hall & Seddougui (1989), subsequently reconsidered by Bassom & Seddougui (1990), has shown that these thin layers are susceptible to

secondary instabilities which take the form of travelling waves confined within these layers. This theoretical investigation, together with the weakly nonlinear account of this form of secondary instability described by Seddougui & Bassom (1991) provides good qualitative agreement with several experimental observations, notably those of Peerhossaini & Wesfreid (1988a,b).

All the work described above has addressed problems which arise when Görtler vortices occur in two-dimensional boundary layers but in many practical situations in which Görtler vortices are known to arise the basic boundary layer is three-dimensional. For example, in the case of a boundary layer flow over a obstacle or the flow over a turbine blade the three-dimensionality of the basic flow is potentially crucial and should not be neglected. Most significantly the development of laminar flow airfoils has given rise to designs which have two areas of concave curvature on the lower side of the airfoil: when the wing is swept the boundary layer flow is fully three-dimensional and the previously mentioned analyses are largely inapplicable.

The first attempt to describe this three-dimensionality effect was given by Hall (1985) who examined the Görtler mechanism in flow over an infinitely long swept cylinder. The results obtained were quite general and did not require a precise description of the particular boundary layer under investigation. In was shown in Hall (1985) that it is the relative size of the crossflow and chordwise flow over the cylinder which is critical in determining the vortex structure. It was demonstrated that as this ratio, say $\lambda^{\dagger}$, was increased from zero the first significant change in the vortex structure from that in the two-dimensional case occurs when $\lambda^{\dagger} \sim R_e^{-\frac{1}{2}}$, where R_e is the (large) Reynolds number defined in (1.1). In this situation the vortices become time dependent and the high wavenumber modes no longer have vortex boundaries aligned with the flow direction. Indeed, as the crossflow increases further, the neutral vortices have axes perpendicular to the vortex lines of the basic flow. The neutral Görtler number for the vortices was predicted by a large wavenumber asymptotic analysis, the results of which suggested that for $O(1)$ values of the ratio of the crossflow and chordwise velocity fields the Görtler mechanism is probably unimportant compared with Tollmien-Schlichting and crossflow type instabilities. Indeed, there is some limited experimental evidence which supports this conclusion. Work by Baskaran & Bradshaw (1988) has shown, at least for turbulent boundary layers, that increasing the crossflow velocity component tends to destroy the Görtler mechanism.

Further investigations concerning the role played by the crossflow component for the Görtler instability was motivated by results obtained by Denier, Hall & Seddougui (1991) (hereafter referred to as DHS). The principal aim of DHS was to provide a

rational theory for the receptivity of Görtler vortices and specifically to explain how the vortices may be triggered by wall roughness elements. In the course of this work, DHS reconsidered the stability of a vortex in a high Görtler number flow by implementing a linear, spatial stability analysis. In particular, for $G \gg 1$, they considered the structure of vortices in two different wavenumber regimes: they reworked the analysis of Hall (1982a) for high $O\left(G^{\frac{1}{4}}\right)$ wavenumbers and also examined O(1) wavenumber vortices. This latter disturbance mode is governed by inviscid equations. By considering the region between these two wavenumber regimes DHS identified a new structure which is relevant for vortices of wavenumber $O\left(G^{\frac{1}{5}}\right)$ and which has the property that the vortices are trapped in a thin layer of thickness $O\left(G^{-\frac{1}{5}}\right)$ at the wall. Furthermore DHS showed that within this $O\left(G^{\frac{1}{5}}\right)$ wavenumber regime there exists a unique most unstable Görtler vortex according to linear stability theory.

Bassom & Hall (1991) (hereafter referred to as BH) extended the work of DHS to consider the effect of introducing crossflow into the boundary layer flow. Like DHS, BH conducted a spatial stability analysis of the vortex modes and they demonstrated that for O(1) wavenumber modes at large Görtler numbers the crossflow first has significant effects on the two-dimensional results once this parameter becomes $O(R_e^{-\frac{1}{2}} G^{\frac{1}{2}})$. As the crossflow increases the stationary vortex structure takes on an identity which is essentially that of a crossflow instability; a mechanism first investigated by Gregory, Stuart & Walker (1955). BH surmised that for certain values of crossflow there are ranges of O(1) wavenumber space such that vortices with wavenumbers within these bands cannot persist. The work contained in BH and concerned with these essentially inviscid modes has been subsequently extended on two fronts. First, Dando (1992) considered the effect of allowing for compressibility and has shown that the properties of the modes are sensitive to the value of the Mach number. Second, Bassom (1992) investigated the role of time dependence in the problem and demonstrated that although this effect is important in dictating quantitative properties, it is not significant in affecting the qualitative behaviours of the vortex structures.

The second part of BH was concerned with obtaining a description of the influence of crossflow on the $O(G^{\frac{1}{5}})$ wavenumber (viscous) vortices of DHS. It was shown that when the ratio of crossflow to chordwise flow becomes $O(R_e^{-\frac{1}{2}} G^{\frac{3}{5}})$ the results of DHS need to be modified:- significantly it was demonstrated that the introduction of crossflow into the problem has a stabilising effect, at least according to linear stability theory. In particular, whereas in DHS it was conclusively proved that stationary vortices are necessarily unstable at $O(G^{\frac{1}{5}})$ wavenumbers, this is no longer true once

crossflow terms are introduced. In addition, for certain crossflow values there exist neutrally stable vortex modes whilst at large enough values of the crossflow no vortex structures induced by centrifugal effects can exist. BH also investigated the stability of linearised time–dependent viscous vortices and demonstrated that crossflow also tends to stabilise these modes. Bassom (1992) has since shown how these unsteady viscous modes connect to the corresponding inviscid ones.

The principal aim of the present paper is to extend BH to make a study of the nonlinear stability characteristics of the $O(G^{\frac{1}{5}})$ wavenumber modes elucidated in the latter article. Denier & Hall (1991) have made a numerical study of the nonlinear evolution of these high wavenumber structures within a two–dimensional boundary layer. They showed that the nonlinear equations governing the evolution of the Görtler vortex over an $O(G^{-\frac{3}{5}})$ streamwise lengthscale are fully nonparallel in nature. By implementing the scheme described by Hall (1988), Denier & Hall illustrated that given a suitable initial perturbation then eventually the energy of the higher harmonics grows until a singularity is encountered at some downstream position. It is concluded that it is this singularity which is ultimately the cause of vortices which are originally close to the wall moving into the main part of the boundary layer.

Some work has been initiated concerning the nonlinear stability of the inviscid modes within a three–dimensional boundary layer, Blackaby & Dando (private communication). When results become available from this work they should prove interesting.

In order to make a nonlinear study of the viscous modes we perform an analysis similar in spirit to that performed by Seddougui & Bassom (1991) in their investigation of nonlinear wavy mode instabilities imposed upon large, strongly nonlinear Görtler structures. We have already alluded to the fact that near the right–hand neutral branch for Görtler vortices Hall (1982b) demonstrated that the weakly nonlinear vortex is governed by a mean–field interaction theory as opposed to the more classical Stuart–Watson (1960) type approach. The latter is much more frequently found in nonlinear situations in a variety of fluid mechanics problems. We have noted that BH showed that the effect of increasing the crossflow component of the boundary layer flow is, in general, to stabilise the vortex modes. Indeed there are certain crossflow/ vortex wavenumber pairings which give rise to a neutrally stable structure; this structure is confined to a thin layer adjacent to the curved surface over which the flow occurs. By gradually increasing the amplitude of the vortices from the infinitesimal values upon which linearised theory is based we can identify the crucial vortex size at which nonlinearity becomes important. Like Seddougui & Bassom (1991) we find that at

this point all the harmonics of the disturbance attain asymptotically identical sizes and then the vortex is determined by the solution of an infinity of coupled nonlinear ordinary differential equations.

There have recently been a number of problems studied which share this characteristic that all the harmonics of the spanwise dependence of the vortex play important roles. The resulting infinity of coupled equations poses a formidable numerical challenge in order to execute a satisfactory solution and to our knowledge there have been few attempts to tackle such a problem. One example of such an attempt was made by Bassom & Blennerhassett (1992) who were concerned with obtaining the structure of strongly nonlinear vortices within curved channel flows and they have shown that at sufficiently high Taylor numbers the flow structure develops a wall layer which is of the same size as the vortex wavelength. In this case an infinite–dimensional set of differential equations is obtained, some properties of which were investigated computationally. Earlier work by Denier (1992) concerned with the development of fully nonlinear Taylor vortices has given rise to a similar set of equations but the discussion was restricted to explaining why these equations are guaranteed to have a solution with the desired boundary conditions rather than seeking their solutions explicitly.

Given that the nonlinear development of the high–wavenumber $O(G^{\frac{1}{5}})$ Görtler vortex is governed by the infinity of equations here we address the weakly nonlinear limit. A Stuart–Watson type theory is applicable which leads to an amplitude equation for the evolution of the vortex. Some comments are made concerning the solutions of this equation for a variety of vortex wavenumbers and frequencies. We note here the fact that for these high–wavenumber viscous modes the governing equations may be easily scaled so that the results derived are valid for a wide class of three–dimensional boundary layers. This is in contrast to the situation for the O(1) wavenumber inviscid modes for which the quantitative behaviour of the vortex structures in entirely dependent on the particular boundary layer under consideration.

The remainder of the paper is divided as follows. In the coming section the problem is formulated and the fully nonlinear coupled set of governing differential equations given. The weakly nonlinear limit of these equations is obtained in section 3 and the numerical methods implemented in their solution described in section 4. The nonlinear properties of the modes are given in section 5 and these are then analysed within a low wavenumber limit. We close with some discussion.

§2 Formulation

Our aim is to derive the equations which determine nonlinear high wavenumber viscous vortex modes in a slightly three–dimensional boundary layer. Following Hall (1985) we consider the boundary layer flowing over the cylinder $y = 0$, $-\infty < x < \infty$, where the z–axis is a generator of the cylinder, y is the distance normal to the surface and the x coordinate measures distance along the curved surface. The Reynolds number R_e, the O(1) Görtler number G and the curvature parameter δ are as given in (1.1) where U_0 is a characteristic flow velocity in the x–direction. The basic flow within the three–dimensional boundary layer is assumed to be of the form

$$\mathbf{u} = U_0 \left(\bar{u}(X,Y), R_e^{-\frac{1}{2}} \bar{v}(X,Y), R_e^{-\frac{1}{2}} \lambda^* \bar{w}(X,Y) \right) \left(1 + O\left(R_e^{-\frac{1}{2}} \right) \right) \tag{2.1}$$

where $X = x/l$ and $Y = yR_e^{\frac{1}{2}}/l$, and the crossflow parameter λ^* is of order one. This boundary layer profile is in general found by numerically integrating the downstream momentum and continuity equations to determine $\bar{u}$ and $\bar{v}$, and then finding $\bar{w}$ from the spanwise momentum equation.

It is convenient to define the scaled spanwise coordinate $Z = R_e^{\frac{1}{2}} z/l$ and let t be the temporal variable scaled on l/U_0. The basic velocity profile is perturbed by

$$\left(U(t,X,Y,Z), R_e^{-\frac{1}{2}} V(t,X,Y,Z), R_e^{-\frac{1}{2}} W(t,X,Y,Z) \right), \tag{2.2a}$$

the pressure field is given by

$$p = \bar{p} + R_e^{-1} P(t,X,Y,Z) \tag{2.2b}$$

and on substituting (2.2) into the Navier–Stokes equations then

$$U_X + V_Y + W_Z = 0, \tag{2.3a}$$

$$\begin{aligned} -U_t + U_{YY} + U_{ZZ} - \bar{u}_Y V - \bar{u} U_X - \bar{u}_X U - \bar{v} U_Y - \lambda^* \bar{w} U_z \\ = U U_X + V U_Y + W U_Z, \end{aligned} \tag{2.3b}$$

$$\begin{aligned} -V_t + V_{YY} + V_{ZZ} - G\chi \bar{u} U - P_Y - \bar{u} V_X - \bar{v}_X U - \bar{v} V_Y - \bar{v}_Y V - \lambda^* \bar{w} V_z \\ = U V_X + V V_Y + W V_Z + \frac{G}{2} \chi U^2, \end{aligned} \tag{2.3c}$$

$$\begin{aligned} -W_t + W_{YY} + W_{ZZ} - P_Z - \bar{u} W_X - \lambda^* \bar{w}_X U - \bar{v} W_Y - \lambda^* V \bar{w}_Y - \lambda^* \bar{w} W_z \\ = U W_X + V W_Y + W W_Z. \end{aligned} \tag{2.3d}$$

Here terms of relative order $R_e^{-\frac{1}{2}}$ have been neglected.

The linearised solutions studied by BH are obtained by considering (2.3) when all the right hand sides of $(2.3b-d)$ are put equal to zero. Additionally, the nonlinear equations examined by Denier & Hall (1991) to determine the development of large vortices in two-dimensional boundary layers can be retrieved by setting $\lambda^* = 0$ in the above.

We now follow the scalings first derived by DHS in which it was shown that the $O(G^{\frac{1}{5}})$ wavenumber vortices are confined to a layer of thickness $O(G^{-\frac{1}{5}})$ adjacent to the cylinder. These modes have a spatial growth rate $O(G^{\frac{3}{5}})$, and it was proved in BH that the three-dimensionality of the basic flow is first significant for these viscous vortices once the scaled crossflow λ^* is $O(G^{\frac{3}{5}})$. Therefore it is convenient to define the O(1) crossflow parameter $\hat{\lambda}$ by

$$\lambda^* = G^{\frac{3}{5}}\hat{\lambda}. \tag{2.4a}$$

If the spanwise wavenumber of the fundamental vortex is taken to be a (which, recall, is $O(G^{\frac{1}{5}})$) then the scaled wavenumber k_0 is defined according to

$$a = k_0 G^{\frac{1}{5}}, \tag{2.4b}$$

and the disturbance is confined to the region where the co-ordinate ψ given by

$$\psi = k_0 G^{\frac{1}{5}} Y, \tag{2.4c}$$

is of order one. In this layer the nonlinear disturbance assumes the form

$$U = \Delta G^{-\frac{1}{5}} \left(\sum_{n=-\infty}^{n=\infty} U_{0n} E_1^n + G^{-\frac{1}{5}} \sum_{n=-\infty}^{n=\infty} U_{1n} E_1^n + \ldots \right), \tag{2.5a}$$

$$V = \Delta G^{\frac{1}{5}} \left(\sum_{n=-\infty}^{n=\infty} V_{0n} E_1^n + G^{-\frac{1}{5}} \sum_{n=-\infty}^{n=\infty} V_{1n} E_1^n + \ldots \right), \tag{2.5b}$$

$$W = \Delta G^{\frac{2}{5}} \left(\sum_{n=-\infty}^{n=\infty} W_{0n} E_1^n + G^{-\frac{1}{5}} \sum_{n=-\infty}^{n=\infty} W_{1n} E_1^n + \ldots \right), \tag{2.5c}$$

$$P = \Delta G^{\frac{2}{5}} \left(\sum_{n=-\infty}^{n=\infty} P_{0n} E_1^n + G^{-\frac{1}{5}} \sum_{n=-\infty}^{n=\infty} P_{1n} E_1^n + \ldots \right), \tag{2.5d}$$

where

$$E_1 \equiv \exp\left[ik_0 G^{\frac{1}{5}} Z + G^{\frac{4}{5}} \int^X \left(\beta_0 + G^{-\frac{1}{5}}\beta_1(X) + \ldots\right) dX \right.$$
$$\left. -iG^{\frac{2}{5}} \int^t (\Omega_0(t) + G^{-\frac{1}{5}}\Omega_1(t) + \ldots)dt\right]. \qquad (2.5e)$$

This definition of E_1 reflects the fact that the vortex has spanwise wavenumber $O(G^{\frac{1}{5}})$ and that the results of BH demonstrate that the disturbance has an $O(G^{\frac{3}{5}})$ growth rate (since it transpires that β_0 is purely imaginary). Furthermore, the parameter Δ is at our disposal. Initially the choice $\Delta = 1$ is made which permits the fully nonlinear vortex equations to be deduced but subsequently Δ is allowed to tend to zero which corresponds to taking the appropriate weakly nonlinear limit.

For $Y \ll 1$ the basic flow quantities $\bar{u}$, $\bar{w}$ are assumed to take the forms

$$\overline{u} = \mu_{11}(X)Y + \frac{\mu_{12}(X)}{2!}Y^2 + \frac{\mu_{13}(X)}{3!}Y^3 + \cdots, \qquad (2.6a)$$

$$\overline{w} = \mu_{21}(X)Y + \frac{\mu_{22}(X)}{2!}Y^2 + \frac{\mu_{23}(X)}{3!}Y^3 + \cdots, \qquad (2.6b)$$

and $\overline{v} = O(Y^2)$. The vortex equations are now derived by substituting (2.4–6) in equations (2.3) and comparing coefficients of like terms. The continuity equation (2.3a) yields

$$\beta_0 U_{0n} + ik_0 W_{0n} = 0, \qquad \text{if} \quad n \neq 0 \qquad (2.7a)$$

$$V_{00} = 0, \qquad (2.7b)$$

$$n(\beta_1 U_{0n} + \beta_0 U_{1n} + ik_0 W_{1n}) + k_0 \frac{dV_{0n}}{d\psi} = 0. \qquad (2.7c)$$

The streamwise and spanwise momentum equations (2.3b, d) then give

$$\beta_0 U_{00} + ik_0 W_{00} = -\left(\frac{\beta_0 \mu_{11}}{k_0} + i\hat{\lambda}\mu_{21}\right)\psi, \qquad (2.8)$$

but the constraint that the disturbance be confined to the thin wall layer requires that U_{00}, W_{00} remain bounded as $\psi \to \infty$ which in turn forces the relationship

$$\frac{\beta_0 \mu_{11}}{k_0} + i\hat{\lambda}\mu_{21} = 0. \qquad (2.9a)$$

This confirms the assertion that β_0 is purely imaginary and then (2.8) becomes

$$\beta_0 U_{00} + ik_0 W_{00} = 0. \qquad (2.9b)$$

Next order terms in the streamwise momentum equation leads to the equation

$$\left(\frac{d^2}{d\psi^2} - N^2 + \frac{i\Omega_0 N}{k_0^2} - \frac{\beta_1\mu_{11}}{k_0^3}N\psi - \frac{i\hat{\lambda}\left(\mu_{11}\mu_{22}-\mu_{12}\mu_{21}\right)}{2k_0^3\mu_{11}}N\psi^2\right)U_{0N} - \frac{\mu_{11}}{k_0^2}V_{0N}$$
$$= \frac{1}{k_0}\sum_{n=-\infty,n\neq N}^{\infty}\left(\frac{dU_{0n}}{d\psi}V_{0(N-n)} - \frac{n}{N-n}U_{0n}\frac{dV_{0(N-n)}}{d\psi}\right)$$
$$+ \frac{NU_{0N}}{k_0^2}\left(\beta_0 U_{10} + \beta_1 U_{00} + ik_0 W_{10}\right). \tag{2.10}$$

Our aim is to derive the governing equations for the leading order vortex components $\{U_{0n}, V_{0n}\}$. Clearly one relation between these unknowns is established by (2.10) once an expression for $(\beta_0 U_{10} + \beta_1 U_{00} + ik_0 W_{10})$ is found. Third order components of momentum equations $(2.3b,d)$ may be combined to show that if

$$\hat{\Phi} = \beta_0 U_{10} + ik_0 W_{10}, \tag{2.11a}$$

then

$$\frac{d^2\hat{\Phi}}{d\psi^2} = \frac{1}{k_0}\frac{d}{d\psi}\left(\sum_{n=-\infty,n\neq 0}^{\infty}\left(\left(\beta_0 U_{1n} + ik_0 W_{1n}\right)V_{0(-n)}\right)\right). \tag{2.11b}$$

Employing relation $(2.7c)$ and using (2.10) for $N = 0$ gives

$$\left(\beta_0 U_{10} + \beta_0 U_{00} + ik_0 W_{10}\right) = -\sum_{n=-\infty,n\neq 0}^{\infty}\frac{1}{n}\left(\int_0^{\psi}\frac{dV_{0n}}{d\psi}V_{0(-n)}d\psi\right),$$

which in turn reduces (2.10) to

$$\left(\frac{d^2}{d\psi^2} - N^2 + \frac{i\Omega_0 N}{k_0^2} - \frac{\beta_1\mu_{11}}{k_0^3}N\psi - \frac{i\hat{\lambda}\left(\mu_{11}\mu_{22}-\mu_{12}\mu_{21}\right)}{2k_0^3\mu_{11}}N\psi^2\right)U_{0N} - \frac{\mu_{11}}{k_0^2}V_{0N}$$
$$= \frac{1}{k_0}\sum_{n=-\infty,n\neq N}^{\infty}\left(\frac{dU_{0n}}{d\psi}V_{0(N-n)} - \frac{n}{N-n}U_{0n}\frac{dV_{0(N-n)}}{d\psi}\right)$$
$$- \frac{NU_{0N}}{k_0^2}\sum_{n=-\infty,n\neq 0}^{\infty}\frac{1}{n}\left(\int_0^{\psi}\frac{dV_{0n}}{d\psi}V_{0(-n)}d\psi\right). \tag{2.12}$$

The second equation for the leading order vortex components is obtained by following the scheme outlined in BH. Order $G^{\frac{4}{5}}$ terms in the $Y-$ momentum equation

(2.3c) enables a relation for the leading order pressure gradient to be derived in the form

$$\frac{dP_{0N}}{d\psi} = k_0\left(\frac{d^2}{d\psi^2} - N^2 + \frac{i\Omega_0 N}{k_0^2} - \frac{\beta_1\mu_{11}}{k_0^3}N\psi - \frac{i\hat{\lambda}(\mu_{11}\mu_{22}-\mu_{12}\mu_{21})}{2k_0^3\mu_{11}}N\psi^2\right)V_{0N}$$
$$- \frac{\mu_{11}\chi_0\psi}{k_0^2}U_{0N} - \frac{NV_{0N}}{k_0}\left(\beta_0 U_{10} + \beta_1 U_{00} + ik_0 W_{10}\right)$$
$$- \sum_{n=-\infty, n\neq N}^{\infty}\left(\frac{dV_{0n}}{d\psi}V_{0(N-n)} - \frac{n}{N-n}V_{0n}\frac{dV_{0(N-n)}}{d\psi}\right) - \frac{\chi_0}{2k_0}\sum_{-\infty}^{\infty}U_{0n}U_{0(N-n)}. \tag{2.13}$$

Also $O(G^{\frac{1}{5}})$ and $O(G^{\frac{4}{5}})$ terms in the streamwise momentum equation (2.3b) and the spanwise momentum equation (2.3d) respectively show that

$$\left[\frac{d^2}{d\psi^2} - N^2 + \frac{i\Omega_0 N}{k_0^2} - \frac{\beta_1\mu_{11}N\psi}{k_0^3} - \frac{i\hat{\lambda}(\mu_{11}\mu_{22}-\mu_{21}\mu_{12})N\psi^2}{2k_0^3\mu_{11}}\right]U_{1N}$$
$$- \frac{\mu_{11}V_{1N}}{k_0^2} = RHS_1, \tag{2.14a}$$

and

$$\left[\frac{d^2}{d\psi^2} - N^2 + \frac{i\Omega_0 N}{k_0^2} - \frac{\beta_1\mu_{11}N\psi}{k_0^3} - \frac{i\hat{\lambda}(\mu_{11}\mu_{22}-\mu_{21}\mu_{12})N\psi^2}{2k_0^3\mu_{11}}\right]W_{1N}$$
$$- \frac{\hat{\lambda}\mu_{21}V_{1N}}{k_0^2} - \frac{iN}{k_0}P_{0N} = RHS_2, \tag{2.14b}$$

where the complicated terms RHS_1 and RHS_2 involve $\{U_{0n}, V_{0n}\}$. By adding β_0 multiples of (2.14a), ik_0 multiples of (2.14b) and β_1 multiples of (2.12), differentiating the resulting equation with respect to ψ and substituting for $dP_{0N}/d\psi$ according to (2.13) leads to the required second equation relating the leading order vortex quantities.

As in BH it is convenient to invoke the scalings

$$k_0 = \left(\chi_0\mu_{11}^2\right)^{\frac{1}{5}}k, \qquad \hat{\beta} = i\chi_0^{\frac{3}{5}}\mu_{11}^{\frac{1}{5}}\beta, \qquad U_{0N} = \chi_0^{-\frac{1}{5}}\mu_{11}^{\frac{3}{5}}U_N, \tag{2.15a-c}$$

$$V_{0N} = \chi_0^{\frac{1}{5}}\mu_{11}^{\frac{2}{5}}V_N, \qquad \Omega_0 = -\chi_0^{\frac{2}{5}}\mu_{11}^{\frac{4}{5}}\Omega, \tag{2.15d-e}$$

$$\hat{\Phi} = \chi_0^{\frac{2}{5}}\mu_{11}^{\frac{4}{5}}\Phi, \qquad \lambda = \frac{\hat{\lambda}(\mu_{11}\mu_{22}-\mu_{21}\mu_{12})}{2\mu_{11}^{\frac{1}{5}}\chi_0^{\frac{3}{5}}}, \tag{2.15f-g}$$

which reduce the pair of equations for the vortex to the forms

$$\left(\frac{d^2}{d\psi^2} - N^2 - \frac{i\Omega N}{k^2} - \frac{i\beta N\psi}{k^3} - \frac{i\lambda N\psi^2}{k^3}\right) U_N - \frac{V_N}{k^2}$$
$$= \frac{1}{k}\sum_{n=-\infty, n\neq N}^{\infty}\left(\frac{dU_n}{d\psi}V_{N-n} - \frac{n}{N-n}U_n\frac{dV_{N-n}}{d\psi}\right) + \frac{NU_N\Phi}{k^2}, \tag{2.16a}$$

where

$$\Phi \equiv -\int_0^{\psi}\left(\sum_{n=-\infty, n\neq 0}^{\infty}\frac{1}{n}\frac{dV_n}{d\psi}V_{-n}\right)d\psi, \tag{2.16b}$$

and

$$\left(\frac{d^2}{d\psi^2} - N^2 - \frac{i\Omega N}{k^2} - \frac{i\beta N\psi}{k^3} - \frac{i\lambda N\psi^2}{k^3}\right)\left(\frac{d^2}{d\psi^2} - N^2\right)V_N + \frac{2i\lambda N}{k^3}V_N + \frac{N^2\psi}{k^3}U_N$$
$$= \frac{N}{k^2}\left(\Phi\left(\frac{d^2}{d\psi^2} - N^2\right)V_N - V_N\frac{d^2\Phi}{d\psi^2}\right) - \frac{N^2}{2k^2}\sum_{-\infty}^{\infty}U_nU_{N-n}$$
$$- \frac{1}{k}\sum_{n=-\infty, n\neq 0, N}^{\infty}\left(\frac{N^2(2n-N)}{n}\frac{dV_n}{d\psi}V_{N-n} + \frac{N^2}{n}\frac{dV_n}{d\psi}\frac{d^2V_{N-n}}{d\psi^2} - \frac{N}{n}V_{N-n}\frac{d^3V_n}{d\psi^3}\right). \tag{2.16c}$$

Notice that the scaling (2.15*b*) ensures that neutrally stable modes correspond to the case when the scaled parameter β is purely real valued.

These equations dictate the strongly nonlinear evolution of vortex modes and are the three-dimensional extensions those equations solved by Denier & Hall (1991). A numerical solution of the full three-dimensional equations (2.16) is planned for a future paper but for present attention is restricted to the consideration of the weakly nonlinear properties of these equations. Such a treatment enables predictions to be made concerning the properties of Görtler vortices in three-dimensional boundary layers of practical importance. It is to be noted that the scalings (2.15) ensure that the ensuing deductions may be related to a wide variety of boundary layers and the precise properties of vortices within any particular flow may be easily deduced by appealing to the recipes (2.15) with the particular boundary layer functions χ_0, μ_{11}, μ_{12}, μ_{21} and μ_{22} inserted.

Consequently, in the following section we concentrate on the case when $|U_N|$ and $|V_N|$ are small or, equivalently, in the context of the original expansions (2.5), when the parameter $\Delta \ll 1$.

§3 The weakly nonlinear theory

Our analysis of the full equations (2.16) is concerned with the problem in which the vortex mode is of amplitude $O(h)$, with $h \ll 1$, relative to the scalings implied in (2.5). In this case, in keeping with the usual weakly nonlinear approach we anticipate from (2.16) that the perturbation quantities are changed by $O(h^2)$ from their linear values and so

$$U_1 = h\hat{U}_{10} + h^3\hat{U}_{11}\cdots, \qquad V_1 = h\hat{V}_{10} + h^3\hat{V}_{11} + \cdots, \tag{3.1a,b}$$

$$U_2 = h^2\hat{U}_{20} + \cdots, \qquad V_2 = h^2\hat{V}_{20} + \cdots, \tag{3.1c,d}$$

$$U_0 = h^2\hat{U}_{00} + \cdots, \qquad \Phi = h^2\hat{\Phi}_0 + \cdots, \tag{3.1e,f}$$

and the scaled parameters involved take the forms

$$\beta = \beta_0 + h^2\beta_2 + \cdots, \qquad \Omega = \Omega_0 + h^2\Omega_2 + \cdots. \tag{3.1g,h}$$

The remaining terms in (2.16) are sufficiently small so as to become negligible in the ensuing analysis.

The expressions (3.1) when inserted in (2.16) suggest that it is convenient to define the operator L_N by

$$L_N \equiv \frac{d^2}{d\psi^2} - N^2 - \frac{i\Omega_0 N}{k^2} - \frac{i\beta_0 N\psi}{k^3} - \frac{i\lambda N\psi^2}{k^3}. \tag{3.2}$$

At leading order in (2.16) we obtain the system

$$L_1\left(\hat{U}_{10}\right) - \frac{\hat{V}_{10}}{k^2} = 0, \tag{3.3a}$$

$$L_1\left(\frac{d^2}{d\psi^2} - 1\right)\hat{V}_{10} + \frac{2i\lambda}{k^3}\hat{V}_{10} = -\frac{\psi}{k^3}\hat{U}_{10}, \tag{3.3b}$$

which needs to be solved subject to the conditions

$$\hat{U}_{10}, \quad \hat{V}_{10}, \quad \frac{d\hat{V}_{10}}{d\psi} \longrightarrow 0 \qquad \text{as} \quad \psi \longrightarrow 0, \infty, \tag{3.3c}$$

in order to ensure zero disturbance quantities on the surface $Y = 0$ and that the vortex decays as $Y \longrightarrow \infty$. The system (3.3) is, of course, just the linear viscous equations discussed in BH. The salient properties of the relevant solutions of (3.3) will be discussed in a forthcoming section.

At $O(h^2)$ in equations (2.16) it is found that $\hat{U}_{00}$ and $\hat{\Phi}_0$ satisfy

$$\hat{U}_{00} = \int_0^{\psi} \frac{1}{k}(\hat{U}_{10}\hat{V}_{10}^* + \hat{U}_{10}^*\hat{V}_{10})d\psi, \qquad \hat{\Phi}_0 = \int_0^{\psi} \left(\hat{V}_{10}\frac{d\hat{V}_{10}^*}{d\psi} - \hat{V}_{10}^*\frac{d\hat{V}_{10}}{d\psi} \right) d\psi, \quad (3.4)$$

where here, and in the remainder of this article, an asterisk used as a superscript on a quantity denoted the complex conjugate of that quantity. Also, at the same order, the harmonic terms $\hat{U}_{20}$ and $\hat{V}_{20}$ are determined by the pair

$$L_2\left(\hat{U}_{20}\right) - \frac{\hat{V}_{20}}{k^2} = \frac{1}{k}\left(\frac{d\hat{U}_{10}}{d\psi}\hat{V}_{10} - \hat{U}_{10}\frac{d\hat{V}_{10}}{d\psi} \right), \quad (3.5a)$$

$$L_2\left(\frac{d^2}{d\psi^2} - 4\right)\hat{V}_{20} + \frac{4i\lambda}{k^3}\hat{V}_{20} + \frac{4\psi}{k^3}\hat{U}_{20} = \frac{2}{k}\left(\hat{V}_{10}\frac{d^3\hat{V}_{10}}{d\psi^3} - 2\frac{d\hat{V}_{10}}{d\psi}\frac{d^2\hat{V}_{10}}{d\psi^2} \right) - \frac{2}{k^2}\hat{U}_{10}^2, \quad (3.5b)$$

subject to the boundary conditions that

$$\hat{U}_{20}, \quad \hat{V}_{20}, \quad \frac{d\hat{V}_{20}}{d\psi} \longrightarrow 0 \qquad \text{as} \quad \psi \longrightarrow 0, \infty. \quad (3.5c)$$

The numerical procedures implemented in order to solve (3.3) and (3.5) are described in the coming section and so here we concentrate on deriving the required amplitude equation. In order to obtain the desired equation then it is necessary to consider $O(h^3)$ terms in (2.16) which lead to the pair

$$L_1\left(\hat{U}_{11}\right) - \frac{\hat{V}_{11}}{k^2} = \left(\frac{i\Omega_2}{k^2} + \frac{i\beta_2\psi}{k^3}\right)\hat{U}_{10} + \frac{1}{k}\left(\frac{d\hat{U}_{10}^*}{d\psi}\hat{V}_{20} + \frac{d\hat{U}_{00}}{d\psi}\hat{V}_{10} + \frac{d\hat{U}_{20}}{d\psi}\hat{V}_{10}^* + \frac{\hat{U}_{10}^*}{2}\frac{d\hat{V}_{20}}{d\psi} + 2\hat{U}_{20}\frac{d\hat{V}_{10}^*}{d\psi} \right) + \frac{\hat{U}_{10}\hat{\Phi}_0}{k^2}, \quad (3.6a)$$

$$L_1\left(\frac{d^2}{d\psi^2} - 1\right)\hat{V}_{11} + \frac{2i\lambda}{k^3}\hat{V}_{11} + \frac{\psi\hat{U}_{11}}{k^3} = \left(\frac{i\Omega_2}{k^2} + \frac{i\beta_2\psi}{k^3}\right)\left(\frac{d^2}{d\psi^2} - 1\right)\hat{V}_{10}$$
$$+ \frac{1}{k^2}\left(\hat{\Phi}_0\left(\frac{d^2}{d\psi^2} - 1\right)\hat{V}_{10} - \hat{V}_{10}\frac{d^2\hat{\Phi}_0}{d\psi^2} - \hat{U}_{10}^*\hat{U}_{20} - \hat{U}_{00}\hat{U}_{10} \right)$$
$$- \frac{1}{k}\left(3\hat{V}_{20}\frac{d\hat{V}_{10}^*}{d\psi} + \frac{3}{2}\hat{V}_{10}^*\frac{d\hat{V}_{20}}{d\psi} - \frac{d\hat{V}_{10}^*}{d\psi}\frac{d^2\hat{V}_{20}}{d\psi^2} + \frac{1}{2}\frac{d\hat{V}_{20}}{d\psi}\frac{d^2\hat{V}_{10}^*}{d\psi^2} + \hat{V}_{20}\frac{d^3\hat{V}_{10}^*}{d\psi^3} - \frac{\hat{V}_{10}^*}{2}\frac{d^3\hat{V}_{20}}{d\psi^3} \right), \quad (3.6b)$$

subject to the boundary conditions

$$\hat{U}_{11}, \quad \hat{V}_{11}, \quad \frac{d\hat{V}_{11}}{d\psi} \longrightarrow 0 \qquad \text{as} \quad \psi \longrightarrow 0, \infty. \tag{3.6c}$$

The homogeneous form of (3.6) is merely (3.3) and so, as is the normal method within a weakly nonlinear analysis, equations (3.6) only have a suitable solution if a certain compatibility condition is satisfied. This condition leads to the specification of the correction terms β_2 and Ω_2 within the streamwise dependence and frequency expansions detailed by $(3.1g,h)$. To derive the compatibility requirement it is necessary to first consider the system adjoint to the homogeneous equations (3.3). This adjoint system consists of the functions $\hat{F}(\psi)$ and $\hat{G}(\psi)$ which are the solutions of the coupled equations

$$L_1\left(\hat{F}\right) + \frac{\psi}{k^3}\hat{G} = 0, \tag{3.7a}$$

$$\begin{aligned}\frac{d^4\hat{G}}{d\psi^4} - \left(2 + \frac{i\Omega_0}{k^2} + \frac{i\beta_0\psi}{k^3} + \frac{i\lambda\psi^2}{k^3}\right)\frac{d^2\hat{G}}{d\psi^2} - \left(\frac{2i\beta_0}{k^3} + \frac{4i\lambda\psi}{k^3}\right)\frac{d\hat{G}}{d\psi} \\ + \left(\frac{i\lambda\psi^2}{k^3} + \frac{i\beta_0\psi}{k^3} + \frac{i\Omega_0}{k^2} + 1\right)\hat{G} - \frac{\hat{F}}{k^2} = 0,\end{aligned} \tag{3.7b}$$

with the associated conditions that $\hat{F}$, $\hat{G}$ and $d\hat{G}/d\psi \to 0$ as $\psi \to 0, \infty$. Multiplying $(3.6a)$ by $\hat{F}$, $(3.6b)$ by $\hat{G}$, adding and integrating with respect to ψ demonstrates that for a solution of (3.6) to exist necessitates that

$$z_1\beta_2 A + z_2\Omega_2 A = -I_* A|A|^2,$$

where

$$z_1 \equiv \frac{i}{k^3}\int_0^\infty \left(\hat{F}\psi\hat{U}_{10} + \hat{G}\psi\left(\frac{d^2}{d\psi^2} - 1\right)\hat{V}_{10}\right)d\psi, \tag{3.8a}$$

$$z_2 \equiv -\frac{i}{k^2}\int_0^\infty \left(\hat{F}\hat{U}_{10} + \hat{G}\left(\frac{d^2}{d\psi^2} - 1\right)\hat{V}_{10}\right)d\psi, \tag{3.8b}$$

and $I_* \equiv \int_0^\infty H d\psi$, where

$$\begin{aligned}H = &\frac{\hat{F}}{k}\left(\frac{d\hat{U}_{10}^*}{d\psi}\hat{V}_{20} + \frac{d\hat{U}_{00}}{d\psi}\hat{V}_{10} + \frac{d\hat{U}_{20}}{d\psi}\hat{V}_{10}^* + \frac{\hat{U}_{10}^*}{2}\frac{d\hat{V}_{20}}{d\psi} + 2\hat{U}_{20}\frac{d\hat{V}_{10}^*}{d\psi}\right) + \frac{\hat{F}\hat{U}_{10}\hat{\Phi}_0}{k^2} \\ &+ \frac{\hat{G}}{k^2}\left(\hat{\Phi}_0\left(\frac{d^2}{d\psi^2} - 1\right)\hat{V}_{10} - \hat{V}_{10}\frac{d^2\hat{\Phi}_0}{d\psi^2} - \hat{U}_{10}^*\hat{U}_{20} - \hat{U}_{00}\hat{U}_{10}\right) \\ &- \frac{\hat{G}}{k}\left(3\hat{V}_{20}\frac{d\hat{V}_{10}^*}{d\psi} + \frac{3}{2}\hat{V}_{10}^*\frac{d\hat{V}_{20}}{d\psi} - \frac{d\hat{V}_{10}^*}{d\psi}\frac{d^2\hat{V}_{20}}{d\psi^2} + \frac{1}{2}\frac{d\hat{V}_{20}}{d\psi}\frac{d^2\hat{V}_{10}^*}{d\psi^2} + \hat{V}_{20}\frac{d^3\hat{V}_{10}^*}{d\psi^3} - \frac{\hat{V}_{10}^*}{2}\frac{d^3\hat{V}_{20}}{d\psi^3}\right).\end{aligned} \tag{3.8c}$$

Before presenting the results of the computations we observe that the above analysis may be easily generalised so that the vortex evolution on a slow lengthscale and thence the growth or decay of a near neutral disturbance may be monitored. Formally, if we consider the neighbourhood of the point $X = X_n$ (the point at which an infinitesimal vortex is neutrally stable) and allow a constant frequency disturbance to develop on a lengthscale $\tilde{X}$ where $\tilde{X} = G^{-\frac{3}{5}} h^{-2}(X - X_n)$ with $h \ll 1$, then the result of repeating the previous analysis for a disturbance of amplitude $hA(\tilde{X})$ relative to the scalings implied in (2.5) is the evolution equation

$$\frac{dA}{d\tilde{X}} = \left(-\frac{iz_2}{z_1}\right)\Omega_2 A - \left(\frac{iI_*}{z_1}\right) A|A|^2, \tag{3.9a}$$

It is then simple to derive the equation for the vortex amplitude

$$\frac{d}{d\tilde{X}}\left(|A|^2\right) = c_1\Omega_2|A|^2 + c_2|A|^4, \tag{3.9b}$$

where

$$c_1 \equiv 2Re\left(-\frac{iz_2}{z_1}\right), \qquad c_2 \equiv 2Re\left(-\frac{iI_*}{z_1}\right). \tag{3.9c,d}$$

In order to evaluate the coefficients in (3.9*b*) it is necessary to solve the systems (3.3–5) and (3.7) so that the expressions for z_1, z_2 and I_* as defined in (3.8) may be found. Several limits are of interest: in particular we discuss asymptotic explanations of the properties of solutions of equation (3.9*b*) for situations of large or small scaled vortex wavenumber k as defined in (2.4*b*) and (2.15*a*).

It is clear that if $(\Omega_0, \beta_0, \lambda)$ is an eigenset of (3.3) then so is $(-\Omega_0^*, -\beta_0^*, -\lambda)$ for real crossflows λ. Evidently, it is possible to restrict our attention to positive crossflow parameters without any loss of generality and this is done for the remainder of the paper.

§4 Numerical methods and preliminary calculations

In the context of their work on the viscous vortices BH were solely concerned with the numerical solution of the linear system (3.3). Their computations were based on a technique originally proposed by Malik, Chuang and Hussaini (1982) in which the differential equations to be solved are reduced to a set of linear algebraic equations using either a finite difference discretisation or a spectral representation and the eigenvalues found by solving the characteristic determinant of a generalised eigenvalue problem. The particular method described in Malik *et al.* uses a fourth order accurate (Euler-Maclaurin) finite difference scheme with nodal points distributed so as to resolve any

singular layers and was implemented in order to examine the temporal and spatial stability of a three– dimensional compressible boundary layer flow over a swept wing.

For the present work we attempted to adapt the methods used by BH but eventually concluded that we needed to use a more efficient algorithm here. The reasons for reaching this conclusion were twofold:- first the form of the code relevant to the linearised problem (3.3) does not lend itself to easy modification for use in inhomogeneous problems such as (3.5). Second, and perhaps more importantly, BH conducted a small number of computations of solutions to (3.3) restricted to the three scaled frequency choices $\Omega_0 = 1, 0, -1$. (This was due to limits on the available computing resources.) In order to execute the additional calculations required to compute the amplitude equation coefficients c_1 and c_2 as defined in (3.9) and to extend the results to a greater frequency range it was felt that an improved algorithm was required. We mention in passing that there was an unexpected by–product of using the improved scheme as it enabled us to explain certain of the computational difficulties encountered by both BH and Bassom (1992) and which are described later.

We first detail our computational technique as far as it applies to solving the homogeneous system (3.3). The method has to be adapted for use on non–homogeneous problems (for example (3.5)) and these modifications will be described as required. Therefore we note first that (3.3) can be characterised by the pair of equations

$$\frac{d^4V}{dy^4} + \hat{\alpha}_v \frac{d^2V}{dy^2} + \hat{\beta}_v \frac{dV}{dy} + \hat{\gamma}_v V + \hat{\delta}_v U = 0, \tag{4.1a}$$

$$\frac{d^2V}{dy^2} + \hat{\alpha}_u U + \hat{\beta}_u V = 0, \tag{4.1b}$$

where the coefficients $\hat{\alpha}_u$, $\hat{\alpha}_v, \ldots$ etc. are known functions of y.

The system comprising of (4.1) with associated boundary conditions typified by (3.3c) is an eigenvalue problem and was solved by considering (4.1) with only five of the homogeneous boundary conditions invoked. In addition a normalisation constraint was imposed so that (4.1) was solved subject to

$$U = V = 0, \qquad \frac{dU}{dy} = 1 \qquad \text{at} \qquad y = 0, \tag{4.2a}$$

$$U = V = \frac{dV}{dy} \to 0 \qquad \text{as} \qquad y \to \infty. \tag{4.2b}$$

Iteration on the eigenvalue ensured that the sixth boundary condition $dV/dy = 0$ at $y = 0$ was satisfied. Specifically, in the context of problem (3.3), system (4.1–2)

was solved for complex-valued β_0 for chosen frequency Ω_0, crossflow λ and vortex wavenumber k. Iteration on the imaginary part of β_0 using a Newton iteration to vary λ enabled neutrally stable solutions to be found: cubic splines were used to track along the neutral curves.

As previously mentioned, the main benefit of the present algorithm above that used by BH is the much greater speed of calculation and this is due in part to the implementation of a variable mesh step. The equations (4.1) were discretised using central differencing on the grid y_n, $n = 1, 2, \ldots N$, where $y_1 = 0$ and $y_N = y^{(\infty)}$, where $y^{(\infty)}$ was chosen to be sufficiently large so that the subsequent results were independent of its value. The algorithm permits any grid discretisation, although it was found to be adequate to limit the form to four distinct regions in which the step length was constant: specifically, step length $h = h^{(1)}$ for $0 < y < y^{(1)}$; $h = h^{(j)}$ for $y^{(j-1)} < y < y^{(j)}$, $j = 2, 3, 4$, where $y^{(4)} = y^{(\infty)}$. This grid was found to both resolve both the details of the solution and also integrate over the entire field without using unnecessary steps in the outer region. In all the calculations described henceforth checks were implemented to ensure that the solutions responded smoothly near discontinuity points in the mesh-step size.

Typically this method allowed us to use roughly one-third of the number of points as was required by BH in their implementation of the code described by Malik *et al.* (1982). Further time saving was obtained by formulating our code so as to account for the exact structure of the discretised equations to be solved. The method used in BH may be applied to a much wider variety of boundary value problems whereas the method used here is specific: however we believe that restricting ourselves to such a system specific procedure was worthwhile for with modest grid adaptation we achieved a reduction in computer time to roughly one-thirtieth of that needed by BH. Details of the discretisation used and of the procedure for solving the resulting equations are given in Appendix A.

As a check on the method described above it was decided to repeat some of the linear calculations of BH to ensure consistency. Although BH did conduct a few computations relevant to non neutral infinitesimal modes it should be remembered that our current concern is ultimately with describing the weakly nonlinear modes outlined in section 3: disturbances which by definition are 'close' to the linear neutral stability curve. Therefore effort was concentrated on the neutral modes of BH and figure 1 illustrates such modes for a variety of scaled frequencies Ω_0. BH restricted themselves to the choices $\Omega_0 = 1, 0$ and -1, but the efficiency of the improved algorithm allowed neutral modes to be derived for $\Omega_0 = -2(0.5)3$. Figure 1 shows the crossflow parameter

λ and figure 2 the parameter β_0 as functions of the scaled vortex wavenumber k. We remark that our calculations faithfully reproduced the corresponding findings of BH.

Certain trends surmised by BH on the basis of their numerical work restricted to the three values of Ω_0 are confirmed by our more extensive results. In particular it is seen that neutral modes appear to be possible over wide ranges of the wavenumber and that for large k the crossflow needed to produce neutral modes is quite small. Moreover, DHS illustrated that for $\Omega_0 = \lambda = 0$ all modes within the $O(G^{\frac{1}{5}})$ wavenumber regime are unstable; consequently crossflow is seen to have a stabilising effect. A striking difference also occurs depending upon the sign of the scaled frequency Ω_0. For $\Omega_0 \geq 0$ the neutral modes persist over the complete range of k and as $k \to 0$ the crossflow λ required in order to preserve neutral modes tends to an $O(1)$ value. However for $\Omega_0 < 0$ BH and Bassom (1992) could not find such disturbances for all wavenumbers k and the neutral modes apparently disappeared at some critical k. Figure 1 demonstrates that this critical value increases as Ω_0 becomes more negative, and a possible explanation for this behaviour is given later.

For small wavenumbers k, figure 2 illustrates that the behaviour of the streamwise variation parameter β_0 is also critically dependent upon Ω_0. For $\Omega_0 \geq 0$, as $k \to 0$ then $\beta_0 \to 0$ smoothly (and is proportional to $k^{\frac{1}{2}}$ by the results of BH). A contrasting situation occurs for $\Omega_0 < 0$ for now both λ and β_0 develop erratic behaviours as k decreases; behaviour which was also found in BH. Extensive numerical checks on both our present code and that developed for use in BH were made and confirm these findings.

To conclude this section it is worthwhile to note that the results shown in figure 1 are sufficient to demonstrate that increasing crossflow stabilises the non-stationary vortex modes. There are several regimes in which asymptotic description is possible (in particular those cases of large and small k) but since the primary aim of the present study is to examine the weakly nonlinear system we defer these asymptotic considerations for the present.

§4.1 The weakly nonlinear calculations

Given the outline of the numerical method above the implementation of the routines required to evaluate the amplitude equation coefficients c_1 and c_2 was straightforward and the following methodology was adopted. Once the homogeneous equations (3.3) were solved for the streamwise variation parameter β_0 and scaled crossflow λ in terms of the given frequency Ω_0 and wavenumber k and the respective eigenfunctions

$\hat{U}_{10}$ and $\hat{V}_{10}$ deduced it was a simple matter to evaluate the mean flow quantities $\hat{U}_{00}$ and $\hat{\Phi}_0$ defined in (3.4).

Next the solution of the inhomogeneous system (3.5) was required in order to determine the second harmonic terms $\hat{U}_{20}$ and $\hat{V}_{20}$. Appendix A details the solution strategy for the homogeneous problem but certain modifications are required for dealing with an inhomogeneous case. These are briefly described in Appendix B. Finally, the adjoint functions $\hat{F}(\psi)$ and $\hat{G}(\psi)$ as given by (3.7) were found by using the ideas presented in Appendix A. The integrals z_1 and z_2 as defined in (3.8) were then evaluated using Simpson's rule and the amplitude equation coefficients c_1, c_2 thence deduced. The usual checks were made to ensure the accuracy of the numerical solutions of the systems (3.3), (3.5) and (3.7). In addition, one further check was implemented for each set of solutions; in each system the discretised solutions were substituted into each side of the equations to ensure that the required matrix equations were being solved accurately and that the derived results did indeed solve the problem.

We now consider some properties of the resulting amplitude equation for a variety of parameter choices.

§5 Remarks on the weakly nonlinear properties of the vortex modes

Implementation of the numerical procedures described in section 4 led to the determination of the coefficients c_1 and c_2 appearing in the amplitude equation (3.9*b*). This equation demonstrates that the weak nonlinearity of the problem allows the existence of a threshold equilibrium amplitude A_ϵ given by

$$|A_\epsilon|^2 = -\frac{c_1}{c_2}\Omega_2, \tag{5.1}$$

with $\Omega_2 > 0$ or $\Omega_2 < 0$ as appropriate in order to ensure that the right hand side of (5.1) is positive.

Calculations were conducted for a variety of scaled frequencies Ω_0 taking values between -2 and 3 and the results are summarised in figures 3–5. Figure 3 illustrates the dependence of the coefficient of the linear term in (3.9*b*) (i.e. c_1) upon Ω_0 and the vortex wavenumber k. It is convenient to discuss the cases $\Omega_0 \geq 0$ and $\Omega_0 < 0$ separately. In the former case $c_1 > 0$ across the whole range of wavenumber space which indicates that according to linear theory a mode of frequency $\Omega_0 + h^2\Omega_2$ is unstable for $\Omega_2 > 0$ whereas it is stable for $\Omega_2 < 0$. This is to be expected as from figure 1 it may be deduced that for a fixed crossflow then as the frequency of the mode increases so it loses stability. Furthermore, figure 3 also demonstrates that for $\Omega_0 < 0$

a more erratic behaviour for c_1 occurs. Specifically there are regions of wavenumber space where c_1 just becomes negative and there are rapid variations in c_1 for small k. These changes are easily explained by an asymptotic analysis of the governing systems (3.3), (3.5) and (3.7) for small k: an analysis which is closely allied to work elucidated to in BH and which is explained in section 6. However the small k case for $\Omega_0 < 0$ evolves to a very different structure. Although BH postulated upon the form of this revised configuration they could not solve the resulting equations– the reason for this was surmised by Bassom (1992) as being due to a cut-off point beyond which no neutral solutions could exist. The curves of figure 3 for $\Omega_0 < 0$ lend some credence to this suggestion for as Ω_0 becomes increasingly more negative so the calculations become increasingly more difficult to perform for small k. However, we have also some evidence that a much more elegant computational procedure may lead to a resolution of these difficulties; a matter which is discussed at more length later.

A final comment on figure 3 concerns the wild 'dips' in c_1 observed at relatively large values of k when $\Omega_0 < 0$. This feature is not seen for positive Ω_0 and extensive numerical checks of our work have suggested that this behaviour is real and not just some numerical artefact. As yet we have no convincing argument as to why this behaviour should occur.

We turn now to interpret the findings summarised in figure 4 which illustrates the dependence of coefficient c_2 on k. This coefficient is of greater importance than c_1 for the sign of c_2 reveals the nature of the equilibrium amplitude A_e as defined in (5.1). For all frequencies $\Omega_0 \geq 0$ it is seen that $c_2 < 0$ and consequently the weak nonlinearity of the flow leads to a stabilisation of the vortices. In this case vortices with initial amplitude less than A_e grow to A_e whereas those with initial size greater than A_e tend to diminish. However it must be recalled that if the scaled amplitude A becomes too large the fundamental assumptions underlying weakly nonlinear theory are invalidated and a fully nonlinear account of the vortex structure is essential.

In the main the finding that $c_2 < 0$ also holds for negative scaled frequencies Ω_0. The one additional feature that appears now is the occurence of a large negative spike in the value of c_2 which is evident at a relatively small value of k. Again extensive numerical checks suggest that this is indeed a true feature as opposed to a computational peculiarity. Figures 4e–g also demonstrate that the size of this spike decreases as Ω_0 becomes increasingly more negative.

Finally for this section, equation (5.1) trivially yields information concerning the equilibrium amplitude A_e and which is shown in figure 5 for the various values of Ω_0. Of course many features of this amplitude follow directly from the information

portrayed in figures 3 and 4 and so require little additional comment. We mention first that for all the cases considered $c_2 < 0$ so that modes with perturbed frequency $\Omega_2 > 0$ would be expected to evolve to these equilibrium amplitudes whereas those with $\Omega_2 < 0$ would decay to zero. Again it is convenient to divide our discussion between the cases $\Omega_0 > 0$ and $\Omega_0 < 0$. In the former, as $k \to \infty$, $|A_e| \to 0$ and as k decreases $|A_e|$ rises and reaches a maximum value. As Ω_0 increases so this maximum value decreases. The form of figures 5a–c suggest that for vortices of scaled frequency $\Omega_0 > 0$ those modes with low wavenumbers relative to the $O(G^{\frac{1}{5}})$ implied scaling would be more readily observed than those of greater wavenumber. It should also be noted that as $k \to 0$ the calculations became increasingly sensitive to the grid spacing used and the slight wobbles in the curves as $k \to 0$ are a direst consequence of this.

For Ω_0 negative a number of the trends just described continue to persist. In particular, as Ω_0 moves through increasingly more negative values $|A_e|$ decreases although its maximum value for any fixed frequency occurs at increasing values of k. Again difficulties in evaluation were experienced for small wavenumbers and furthermore, the small values of c_2 as demonstrated in figures 4e–g make computation of $|A_e|$ at large k difficult.

To conclude this description of the weakly nonlinear calculations it is worthwhile to briefly recall the more salient results. Importantly, whereas BH showed that the effect of crossflow is to stabilise the $O(G^{\frac{1}{5}})$ wavenumber modes according to a linearised theory, the above work has demonstrated that crossflow also stabilises the modes on a weakly nonlinear basis. The corresponding equilibrium amplitudes calculated over a range of frequencies and wavenumbers reveals that the largest amplitudes are associated with near stationary vortices and it can be tentatively proposed that these modes are the most likely candidates for practical observation. The analysis originally proposed by BH for small wavenumber linearised vortices at scaled frequencies $\Omega_0 > 0$ may be adapted to allow discussion of these modes using a weakly nonlinear approach and this is considered now.

§6 The low wavenumber ($k \ll 1$) limit for $\Omega_0 > 0$

The calculations presented in BH showed that when $\Omega_0 > 0$, $k \ll 1$ the eigenfunctions $\hat{U}_{10}$ and $\hat{V}_{10}$ of system (3.3) are concentrated in a thin region near $\psi = 0$. They demonstrated that these functions assume a multi-zoned structure form and that the crossflow λ and streamwise variation parameter β_0 required for neutral modes assume the forms

$$\lambda = \lambda_0 + \lambda_1 k^{\frac{1}{4}} + \ldots, \qquad \beta_0 = \beta_{00} k^{\frac{1}{2}} + \beta_{01} k^{\frac{3}{4}} + \ldots, \tag{6.1}$$

where all the constants are real valued. The asymptotic structure for the solution is summarised in figure 6 where it is shown that the configuration divides into a main zone (*II* on figure 6) of thickness $O(k^{\frac{1}{2}})$ which contains a thin region of depth $O(k^{\frac{3}{4}})$, *I*, supplemented by a viscous wall layer of thickness $O(k)$, *III*, and a far field zone, *IV*. It is to be recalled that the normalisation chosen for all the numerical work in this paper is that $\hat{U}'_{10} = 1$ at $\psi = 0$. Guided by this requirement it is easy to adapt the workings of BH to show that the most important contributions to the integrals defined in equations (3.8) occur within the zone *I* wherein it is convenient to write

$$\psi = k^{\frac{1}{2}}\psi_0 + k^{\frac{3}{4}}\left(const. + \hat{\psi}\right). \tag{6.2a}$$

Here $\psi_0 \approx 1.47\Omega_0^{\frac{3}{8}}$ and the constant has a value which is of no concern for the current workings. Furthermore, in zone *I* the solutions $\hat{U}_{10}$ and $\hat{V}_{10}$ develop according to

$$\hat{U}_{10} = k^{-\frac{1}{4}}\hat{\hat{U}}_{10}(\hat{\psi}) + \ldots, \qquad \hat{V}_{10} = k^{\frac{1}{4}}\hat{\hat{V}}_{10}(\hat{\psi}) + \ldots, \tag{6.2b}$$

where these functions satisfy

$$\left(\frac{d^2}{d\hat{\psi}^2} - i\hat{\hat{\Omega}} - i\lambda_0\hat{\psi}^2\right)\hat{\hat{U}}_{10} = \hat{\hat{V}}_{10}, \tag{6.2c}$$

$$\left(\frac{d^2}{d\hat{\psi}^2} - i\hat{\hat{\Omega}} - i\lambda_0\hat{\psi}^2\right)\frac{d^2\hat{\hat{V}}_{10}}{d\hat{\psi}^2} + 2i\lambda_0\hat{\hat{V}}_{10} = -\psi_0\hat{\hat{U}}_{10}, \tag{6.2d}$$

for some constant $\hat{\hat{\Omega}}$ and are subject to the conditions that

$$\hat{\hat{V}}_{10} \longrightarrow \frac{C}{\hat{\psi}}, \qquad \hat{\hat{U}}_{10} \longrightarrow \frac{iC}{\lambda_0\hat{\psi}^3} \quad \text{as} \quad |\hat{\psi}| \to \infty. \tag{6.2e}$$

The constant C is chosen so that $\hat{U}'_{10} = 1$ at $\psi = 0$ and elementary matching between the solutions valid in each of the regions sketched in figure 6 leads to

$$C \approx -0.21i\Omega_0^{\frac{7}{4}}. \tag{6.3}$$

The eigenproblem (6.2) was first solved by Hall (1985) who showed that

$$\psi_0\lambda_0^{-\frac{3}{2}} \approx 4.69, \qquad \hat{\hat{\Omega}}\lambda_0^{-\frac{1}{2}} \approx -2.89,$$

which in turn gives $\lambda_0 \approx 0.46\Omega_0^{\frac{1}{4}}$. This prediction of crossflow required in order to produce neutral modes as $k \to 0$ gives good agreement with the forms depicted in figure 1 for frequencies $\Omega_0 > 0$.

Following this work taken from BH it is straightforward to deduce the forms of the remaining functions within the thin zone I. The adjoint functions are

$$\hat{F} = \hat{\bar{F}}(\hat{\psi}) + \ldots, \qquad \hat{G} = k\hat{\bar{G}}(\hat{\psi}) + \ldots,$$

where

$$\left(\frac{d^2}{d\hat{\psi}^2} - i\hat{\Omega} - i\lambda_0\hat{\psi}^2\right)\hat{\bar{F}} + \psi_0\hat{\bar{G}} = 0, \tag{6.4a}$$

$$\left(\frac{d^2}{d\hat{\psi}^2} - i\hat{\Omega} - i\lambda_0\hat{\psi}^2\right)\frac{d^2\hat{\bar{G}}}{d\hat{\psi}^2} - 4i\lambda_0\hat{\psi}\frac{d\hat{\bar{G}}}{d\hat{\psi}} = \hat{\bar{F}}, \tag{6.4b}$$

subject to the conditions that

$$\hat{\bar{F}} \propto \frac{1}{\hat{\psi}^5} \quad \text{and} \quad \hat{\bar{G}} \propto \frac{1}{\hat{\psi}^3} \quad \text{as} \quad |\hat{\psi}| \to \infty.$$

Furthermore, $U_{20} = k^{-\frac{1}{4}}\hat{U}_{20} + \ldots$, $V_{20} = k^{\frac{1}{4}}\hat{V}_{20} + \ldots$ where $\hat{U}_{20}$ and $\hat{V}_{20}$ are odd-valued functions satisfying

$$\left(\frac{d^2}{d\hat{\psi}^2} - 2i\hat{\Omega} - 2i\lambda_0\hat{\psi}^2\right)\hat{U}_{20} - \hat{V}_{20} = \frac{d\hat{U}_{10}}{d\hat{\psi}}\hat{V}_{10} - \hat{U}_{10}\frac{d\hat{V}_{10}}{d\hat{\psi}}, \tag{6.5a}$$

$$\left(\frac{d^2}{d\hat{\psi}^2} - 2i\hat{\Omega} - 2i\lambda_0\hat{\psi}^2\right)\frac{d^2\hat{V}_{20}}{d\hat{\psi}^2} + 4i\lambda_0\hat{V}_{20} + 4\psi_0\hat{U}_{20} = 2\left(\hat{V}_{10}\frac{d^3\hat{V}_{10}}{d\hat{\psi}^3} - 2\frac{d\hat{V}_{10}}{d\hat{\psi}}\frac{d^2\hat{V}_{10}}{d\hat{\psi}^2}\right), \tag{6.5b}$$

subject to the constraints that $\hat{U}_{20} = O(\hat{\psi}^{-7})$ and $\hat{V}_{20} = O(\hat{\psi}^{-5})$ as $|\hat{\psi}| \to \infty$. Finally, within zone I the functions $\hat{U}_{00}$ and $\hat{\Phi}_0$ are

$$\hat{U}_{00} = k^{-\frac{1}{4}}\hat{\bar{U}}_{00}(\hat{\psi}) + \ldots, \qquad \hat{\Phi}_0 = k^{\frac{1}{4}}\hat{\bar{\Phi}}_{00}(\hat{\psi}) + \ldots,$$

where

$$\hat{U}_{00} = \int_{-\infty}^{\hat{\psi}} \left(\hat{U}_{10}\hat{V}_{10}^{*} + \hat{U}_{10}^{*}\hat{V}_{10} \right) d\hat{\psi} \quad \text{and} \quad \hat{\Phi}_{00} = \int_{-\infty}^{\hat{\psi}} \left(\hat{V}_{10}\frac{d\hat{V}_{10}^{*}}{d\hat{\psi}} - \hat{V}_{10}^{*}\frac{d\hat{V}_{10}}{d\hat{\psi}} \right) d\hat{\psi}. \tag{6.6}$$

Formally, it is possible to use the expansions given above to deduce the forms of the various flow quantities in each of the remaining regions II–IV. However tedious but straightforward manipulations verify that the dominant contributions to the expressions $(3.8a-c)$ arise from within zone I.

The systems (6.2), (6.4) and (6.5) were solved using techniques based upon the general descriptions given in Appendices A and B (some additional remarks specific to these systems are also in the latter Appendix). Simpson's rule was used to evaluate the necessary integrals and thence the amplitude equation coefficients were found to take the forms

$$c_1 \approx 0.7\Omega_0^{-\frac{3}{8}} k^{\frac{1}{4}} + \ldots, \qquad c_2 \approx -7\Omega_0^{\frac{11}{8}} k^3 + \ldots, \tag{6.7a,b}$$

as $k \to 0$. These asymptotic predictions provided reasonable agreement with the numerical results discussed in the preceding section. Results (6.7) then imply that the equilibrium amplitude

$$|A_e| \approx 0.3\Omega_0^{-\frac{7}{8}} k^{-\frac{11}{8}} \sqrt{\Omega_2},$$

which again suggests that it is the low wavenumber relatively low frequency modes which have the greatest equilibrium amplitudes. However there is evidence from figures 5a–c that as k decreases the accuracy of our computational work deteriorates. One difficulty with the prediction of A_e as $k \to 0$ is provided by the extreme smallness of the coefficient c_2 (see (6.7b)). Clearly tiny inaccuracies in the evaluation of c_2 can have drastic consequences for the resulting value of $|A_e|$. As $k \to 0$ it has been demonstrated that the entire solution structure becomes compressed against the wall and then the numerical resolution of the distinct zones sketched in figure 6 is rendered very difficult. Limits on our numerical work were imposed by the available resources and it was considered that it would not be worthwhile to attempt to refine our grid further for reasons described presently.

The scalings described above fail as $\Omega_0 \to 0$ for in this limit the thin layer I moves towards the wall and Bassom (1992) has demonstrated that when $\Omega_0 = O(k^{\frac{4}{7}})$ this layer merges with the viscous wall layer III. Within the wall layer the governing equations now take the forms

$$\left(\frac{d^2}{d\tilde{\xi}^2} - i\tilde{\Omega} - i\tilde{\beta}\tilde{\xi} - i\tilde{\lambda}\tilde{\xi}^2 \right) \tilde{U} = \tilde{V}, \tag{6.8a}$$

$$\left(\frac{d^2}{d\tilde{\xi}^2} - i\tilde{\Omega} - i\tilde{\beta}\tilde{\xi} - i\tilde{\lambda}\tilde{\xi}^2\right)\frac{d^2\tilde{V}}{d\tilde{\xi}^2} + 2i\tilde{\lambda}\tilde{V} = -\tilde{\xi}\tilde{U}, \qquad (6.8b)$$

where the $\tilde{}$ denotes quantities scaled on suitable powers of k (fuller details are given in Bassom (1992)). In particular, $\Omega_0 = k^{\frac{4}{7}}\tilde{\Omega}$ and these wall layer equations need to be solved subject to the conditions that

$$\tilde{U}, \tilde{V} \quad \text{and} \quad \frac{d\tilde{V}}{d\tilde{\xi}} \longrightarrow 0 \quad \text{at} \quad \tilde{\xi} = 0 \quad \text{and as} \quad \tilde{\xi} \to \infty. \qquad (6.8c)$$

Bassom (1992) used the numerical code of Malik *et. al.* (1982) to solve (6.8) for a selection of values of $\tilde{\Omega}$. As $\tilde{\Omega} \to \infty$ he showed how these low frequency modes match with those for which Ω_0 =O(1) but he could only manage to obtain solutions of (6.8) for $\tilde{\Omega}$ greater than $\tilde{\Omega}_c \approx -3.3$. The work of Bassom (1992) was prompted in part by the finding of BH concerning the low wavenumber structure outlined by (6.2) above. The asymptotic regions found by BH are only valid for positive values of Ω_0 and that paper made tentative suggestions concerning possible configurations when $\Omega_0 < 0$. In particular, a critical layer type problem was proposed but no attempt was made to solve this. Subsequent calculations failed to find a solution and Bassom (1992) hoped to connect the $\Omega_0 > 0$ and $\Omega_0 < 0$ cases by investigating the intermediate problem where $\Omega_0 = k^{\frac{4}{7}}\tilde{\Omega}$ by examining the numerical solutions of (6.8) as $\tilde{\Omega} \to -\infty$. However the existence of the cut–off frequency $\tilde{\Omega}_c$ below which numerical solutions were unattainable thwarted this aim.

The system (6.8) was solved using slight modifications to the numerical techniques described in Appendix A. Like Bassom (1992), difficulties were encountered as $\tilde{\Omega}_c$ was approached. Closer studies of this phenomenon revealed that the as $\tilde{\Omega} \to \tilde{\Omega}_c$ the eigensolution migrates from the wall $\tilde{\xi} = 0$ and thus becomes almost completely independent of the boundary conditions imposed at the wall. Therefore the solution becomes insensitive to the values of the eigenparameters and numerical convergence is impossible to obtain. This type of behaviour typically occurs whenever a 'null space' of the system is approached and indicates that the elimination techniques employed to solve the discretised equations need to be replaced by a scheme which directly inverts the entire discretised set (such schemes are termed 'global methods'). This is computationally extremely expensive but it does lead to a determination of a spectrum of eigenvalues of the problem.

This difficulty which arises when a null space of a problem is encountered also provides the explanation for some of the other deficiencies in our numerical work to date. In figures 1 and 2 where neutral curves were presented it is noted that as Ω_0

becomes progressively more negative the wavenumber range over which results were obtained diminishes. Investigations have shown that this is again due to approaching a null space of the appropriate system (3.3).

BH also made some remarks concerning the properties of large wavenumber modes. They demonstrated that as $k \to \infty$ the disturbance remains confined within an O(1) thick region which moves away from $\psi = 0$. Specifically, if $\psi = ck^5 + const. + \psi^\dagger$ (where the precise value of the constant is of no consequence for the leading order problem), $\beta_0 = \beta_{00}k^3 + \ldots$ and $\lambda = \lambda_0 k^{-2} + \ldots$. If the eigenfunctions of (3.3) are written as

$$\hat{U}_{10} = U_0^\dagger + \ldots, \qquad \hat{V}_{10} = k^2 V_0^\dagger + \ldots, \tag{6.9a}$$

then it is easily verified that $\beta_{00} = -\lambda_0 c$ and the eigenfunctions satisfy

$$\left(\frac{d^2}{d\psi^{\dagger 2}} - 1 + \beta_{00}\psi^\dagger\right)\left(\frac{d^2}{d\psi^{\dagger 2}} - 1\right) V_0^\dagger = -cU_0^\dagger, \tag{6.9b}$$

$$\left(\frac{d^2}{d\psi^{\dagger 2}} - 1 + \beta_{00}\psi^\dagger\right) U_0^\dagger = V_0^\dagger. \tag{6.9c}$$

Again BH were unable to solve this eigenproblem for β_{00} and c and it is observed from that paper that calculations of the homogeneous system (3.3) failed for values of k larger than about 1.4. Further researches have once more confirmed that these problems are due to approaching a null space of equations (3.3).

In order to develop our findings of this paper further work is needed to investigate the global numerical methods. Preliminary runs with a small number of grid points have been conducted for the eigenproblem (6.2) first solved by Hall (1985) and for the small frequency problem (6.8) first written down by Bassom (1992). Results for this latter problem have revealed the existence of solutions for $\tilde{\Omega}$ less than the cut-off value $\tilde{\Omega}_c$. This indeed proves that the previous problems for $\tilde{\Omega} < \tilde{\Omega}_c$ are entirely numerically based and have no physical significance. As yet there are too few results from the computationally intensive global method in order to justify a fuller discussion here. However it probable that developments with these ideas will lead to an improved explanation of the large wavenumber and negative Ω_0 limits and we plan to report on our findings in due course.

§7 Discussion and Conclusion

In the previous sections we have described the mechanism by which the introduction of crossflow influences the weakly nonlinear stability characteristics of $O(G^{\frac{1}{5}})$.

wavenumber viscous vortices. The work was confined to the situation in which the crossflow is of size $O(R_e^{-\frac{1}{2}})$ since that is the crucial size at which the crossflow first has a significant effect upon on the vortices. Additionally the Görtler number was taken to be large as this allows non-parallel effects to be accounted for using asymptotic means and, furthermore, is relevant for many realistic boundary layer flows.

One advantage of concentrating on the $O(G^{\frac{1}{5}})$ wavenumber modes, apart from the fact that these are the most unstable for a two-dimensional boundary layer, is that the structure of the disturbance permits all the basic flow quantities which are functions of the particular boundary layer to be scaled out of the problem leaving a system of equations which is valid for a wide variety of three-dimensional flows. Consequently the scalings (2.15) would need to be applied again in order to assess the implications of our findings for any specified flow.

The main conclusion of our work has been that over all the wavenumbers and frequencies investigated the influence of weak nonlinearity is stabilising and the consequent supercritical equilibrium amplitudes have been evaluated. These amplitudes tend to be largest for vortices of small wavenumber and frequencies relative to the initial scalings and suggest that it is these modes which would appear to be the most likely to be observed in practice. A limited asymptotic study has been accomplished which yields indications of the solution characteristics for small k and positive scaled frequencies Ω_0. However the corresponding work for negative Ω_0 and that relevant to large wavenumbers k was not completed due to difficulties in encountering null spaces of the governing differential systems. As reported in the previous section preliminary work has begun using more appropriate numerical methods in order to circumvent these problems. We feel that these calculations are important for the following reason. The work described by BH and that here has conclusively demonstrated that both the linear and weakly nonlinear properties of these viscous vortices are critically dependent upon the sign of the scaled frequency and crossflow λ. For any particular boundary layer either case may be the more relevant (depending upon the signs of the scaling quantities within (2.15)) and so it is desirable that both eventualities are analysed properly. Whereas the solution properties are now reasonably well understood for $\Omega_0 > 0$ this understanding is clearly deficient for $\Omega_0 < 0$ and work on this latter case is continuing.

The other extension of this paper which merits close study is the question as to the nature of the fully nonlinear properties of viscous vortices in three-dimensional boundary layers. The investigation of Denier & Hall (1991) described in the introduction has concentrated upon the two dimensional version of this problem and showed

that in general the vortex suffers a finite distance algebraic breakdown as it develops downstream. Denier & Hall were unable to conduct a weakly nonlinear analysis of the type discussed here for in the two-dimensional boundary layer there are no neutral modes of wavenumber $O(G^{\frac{1}{5}})$. The results of BH and the extensions presented in the current work show that the effect of three-dimensionality is to stabilise the vortex mode. Therefore the three-dimensional version of Denier & Hall (1991) would be most valuable in deciding whether fully nonlinear or crossflow effects are the more important. The former induces a catastrophic breakdown in the flow whereas the latter effect is stabilising and so it can be anticipated that there may well be a delicate balance between the two. It is noted that the full three-dimensional nonlinear equations have already been obtained (in (2.16)) and work is underway to investigate the properties of their solutions.

In the context of our work concerning the viscous modes it should be remembered that a concurrent study by Blackaby & Dando is dedicated to examining the nonlinear properties of O(1) wavenumber inviscid modes whose linear stability properties were outlined in BH. As yet we are not aware of any results arising from their work. Their findings will need to be compared to ours in order for the relative importance of the two nonlinear mode types to be accurately assessed. BH attempted to resolve the question as to which mode is the more likely candidate for practical observation. By carrying out a linearised receptivity calculation of the type given in DHS relevant to Görtler vortices in two-dimensional boundary layers, BH were able to show that wall roughness is a more efficient stimulator of the viscous modes than the inviscid ones and thus the viscous modes might be the easier to generate experimentally. However they also pointed out that as the crossflow increases the growth rates of the inviscid modes increase to become larger than the viscous rates. Thus beyond a certain crossflow size the observed instability may well be a Rayleigh instability as opposed to a centrifugal one.

In many practical situations where Görtler vortices are thought to be a likely cause for transition the basic state is three-dimensional. Our work has demonstrated that a crossflow of small size $O(R_e^{-\frac{1}{2}}G^{\frac{3}{5}})$ is sufficient to stabilise vortex modes according to a weakly nonlinear basis but the results of Denier & Hall (1991) indicate that full nonlinearity of the disturbance may well lead to rapid breakdown. It is a matter of some interest as to the relative importance of these crossflow and nonlinear mechanisms which can only be resolved by extending our findings to the fully nonlinear regime. This problem should obviously be a topic of careful theoretical and practical investigations of the Görtler mechanism in three-dimensional boundary layers.

The authors wish to thank Dr. Craig Streett of NASA Langley for informative guidance regarding the nature of null spaces of the differential systems considered. The research of SRO was supported by the National Aeronautics and Space Administration under NASA contract No. NAS1–18605 while he was in residence at the Institute for Computer Applications in Science and Engineering (ICASE), NASA Langley Research Center, Hampton, VA 23665, USA. APB would like to thank ICASE for their support and hospitality during a visit whilst part of this work was carried out.

APPENDIX A

In this appendix we briefly describe our solution strategy for equations of the general form (4.1).

The derivatives in (4.1) may be discretised as,

$$\frac{d\phi}{dy} = \frac{\phi_{n+1} - \phi_{n-1}}{y_{n+1} - y_{n-1}}, \tag{A1}$$

$$\frac{d^2\phi}{dy^2} = \frac{2\phi_{n+1}}{(y_{n+1} - y_{n-1})(y_{n+1} - y_n)} + \frac{2\phi_n}{(y_{n-1} - y_n)(y_{n+1} - y_n)} + \frac{2\phi_{n-1}}{(y_{n+1} - y_{n-1})(y_n - y_{n-1})}, \tag{A2}$$

and

$$\begin{aligned}\frac{d^4\phi}{dy^4} =& \frac{24\phi_{n+2}}{(y_{n-2} - y_{n+2})(y_{n+1} - y_{n+2})(y_{n+2} - y_{n-1})(y_{n+2} - y_n)} \\ &+ \frac{24\phi_{n+1}}{(y_{n-2} - y_{n+1})(y_{n+1} - y_{n-1})(y_{n+2} - y_{n+1})(y_{n+1} - y_n)} \\ &+ \frac{24\phi_n}{(y_{n-1} - y_n)(y_{n-2} - y_n)(y_n - y_{n+1})(y_n - y_{n+2})} \\ &+ \frac{24\phi_{n-1}}{(y_{n-2} - y_{n-1})(y_{n+1} - y_{n-1})(y_{n+2} - y_{n-1})(y_n - y_{n-1})} \\ &+ \frac{24\phi_{n-2}}{(y_{n-2} - y_{n-1})(y_{n+1} - y_{n-2})(y_{n+2} - y_{n-2})(y_{n-2} - y_n)}.\end{aligned} \tag{A3}$$

Expressions (A1-3) were all obtained by implementing the symbolic manipulation package Mathematica and enable the homogeneous equations (4.1) to be written in the general forms

$$a_n v_{n+2} + b_n v_{n+1} + c_n v_n + d_n v_{n-1} + e_n v_{n-2} + f_n u_n = V_n, \qquad (n = 3, \cdots N-1) \tag{A4a}$$

$$g_n u_{n+1} + h_n u_n + i_n u_{n-1} + j_n v_n = U_n. \qquad (n = 2, \cdots N-1) \tag{A4b}$$

For the homogeneous problem $V_n = U_n = 0$ for all n and the boundary conditions are implemented by imposing

$$u_1 = v_1 = 0, \qquad v_N = u_N = 0,$$

$$\frac{u_2 - u_1}{y_2 - y_1} = 1, \quad \text{(Normalisation)} \qquad \frac{v_{N+1} - v_N}{y_{N+1} - y_N} = 0. \tag{A5}$$

In the context of system (3.3) it remains to ensure that $d\hat{\tilde{V}}_{10}/dy = 0$ at the wall by varying the parameter β. The algorithm employed to solve (A4,5) was an essentially

standard elimination technique. It is convenient to introduce the notation $E_{v,j}$ and $E_{u,j}$ to refer to (A4a) and (A4b) respectively when $n = j$.

The first step is to impose the lower boundary conditions in $E_{u,2}$ by redefining U_2 according to

$$U_2 \to U_2 - h_2 u_2,$$

where $u_2 = u_1 + (y_2 - y_1)\,u' = y_2 - y_1$, since $u = 0$ and $u' = 1$ at $y = 0$. Relations $E_{u,2}$ and $E_{v,3}$ are then solved for v_2 and u_3 and this solution is written as

$$v_2 = \overline{\overline{a}}_{v,2} v_3 + \overline{\overline{b}}_{v,2} v_4 + \overline{\overline{c}}_{v,2} v_5 + \overline{\overline{R}}_{v,2},$$

$$u_3 = \overline{\overline{a}}_{u,3} v_3 + \overline{\overline{b}}_{u,3} v_4 + \overline{\overline{c}}_{u,3} v_5 + \overline{\overline{R}}_{u,3},$$

where

$$\overline{\overline{a}}_{v,2} = -\frac{c_3}{\Gamma_3}, \quad \overline{\overline{b}}_{v,2} = -\frac{b_3}{\Gamma_3}, \quad \overline{\overline{c}}_{v,2} = -\frac{a_3}{\Gamma_3}, \quad \overline{\overline{R}}_{v,2} = \frac{V_3 - \frac{f_3 U_2}{g_2}}{\Gamma_3},$$

$$\overline{\overline{a}}_{u,3} = -\frac{j_2 \overline{\overline{a}}_{v,2}}{g_2}, \quad \overline{\overline{b}}_{u,3} = -\frac{j_2 \overline{\overline{b}}_{v,2}}{g_2}, \quad \overline{\overline{c}}_{u,3} = -\frac{j_2 \overline{\overline{c}}_{v,2}}{g_2}, \quad \overline{\overline{R}}_{u,3} = \frac{U_2}{g_2} - \frac{j_2 \overline{\overline{R}}_{u,3}}{g_2},$$

with $\Gamma_3 = d_3 - f_3 j_2 / g_2$. $E_{u,3}$ is considered next and upon redefining

$$U_3 \to U_3 - i_3 u_2,$$

and eliminating u_3 it is found that

$$g_3 u_4 + j_3 v_3 + \alpha_3 v_4 + \beta_3 v_5 = U_3,$$

where use has been made of the transformations

$$j_3 \to j_3 + h_3 \overline{\overline{a}}_{u,3}, \quad \alpha_3 = h_3 \overline{\overline{b}}_{u,3}, \quad \beta_3 = h_3 \overline{\overline{c}}_{u,3}, \quad U_3 \to U_3 - h_3 \overline{\overline{R}}_{u,3}.$$

Meanwhile v_2 can also be eliminated from $E_{v,4}$ by implementing

$$d_4 \to d_4 + e_4 \overline{\overline{a}}_{v,2}, \quad c_4 \to c_4 + e_4 \overline{\overline{b}}_{v,2}, \quad b_4 \to b_4 + e_4 \overline{\overline{c}}_{v,2}, \quad V_4 \to V_4 - e_4 \overline{\overline{R}}_{v,2}.$$

At this point it is possible to write this procedure in terms of the general equations $E_{v,n}$ and $E_{u,n-1}$. Solving for v_{n-2} and u_{n-1} from $E_{v,n-1}$ and $E_{u,n-2}$, gives

$$v_{n-2} = \overline{\overline{a}}_{v,n-2} v_{n-1} + \overline{\overline{b}}_{v,n-2} v_n + \overline{\overline{c}}_{v,n-2} v_{n+1} + \overline{\overline{R}}_{v,n-2}, \qquad (A6a)$$

$$v_{n-1} = \overline{\overline{a}}_{u,n-1} v_{n-1} + \overline{\overline{b}}_{u,n-1} v_n + \overline{\overline{c}}_{u,n-1} v_{n+1} + \overline{\overline{R}}_{u,n-1}, \qquad (A6b)$$

where

$$\bar{\bar{a}}_{v,n-2} = -\frac{c_{n-1} - \frac{f_{n-1}\alpha_{n-2}}{g_{n-2}}}{\Gamma_{n-1}}, \quad \bar{\bar{b}}_{v,n-2} = -\frac{b_{n-1} - \frac{f_{n-1}\beta_{n-2}}{g_{n-2}}}{\Gamma_{n-1}},$$

$$\bar{\bar{c}}_{v,n-2} = -\frac{a_{n-1}}{\Gamma_{n-1}}, \quad \bar{\bar{R}}_{v,n-2} = \frac{V_{n-1} - \frac{f_{n-1}U_{n-2}}{g_{n-2}}}{\Gamma_{n-1}},$$

and

$$\bar{\bar{a}}_{u,n-1} = -\frac{\alpha_{n-2}}{g_{n-2}} - \frac{j_{n-2}\bar{\bar{a}}_{v,n-2}}{g_{n-2}}, \quad \bar{\bar{b}}_{u,n-1} = -\frac{\beta_{n-2}}{g_{n-2}} - \frac{j_{n-2}\bar{\bar{b}}_{v,n-2}}{g_{n-2}},$$

$$\bar{\bar{c}}_{u,n-1} = -\frac{j_{n-2}\bar{\bar{c}}_{v,n-2}}{g_{n-2}}, \quad \bar{\bar{R}}_{u,n-1} = \frac{U_{n-2}}{g_{n-2}} - \frac{j_{n-2}\bar{\bar{R}}_{v,n-2}}{g_{n-2}}.$$

The unknown u_{n-2} is eliminated from $E_{u,n-1}$ by writing

$$\begin{aligned} \gamma_{n-1} &= i_{n-1}\bar{\bar{a}}_{u,n-2}, \quad j_{n-1} \rightarrow j_{n-1} + i_{n-1}\bar{\bar{b}}_{u,n-2}, \\ \alpha_{n-1} &= i_{n-1}\bar{\bar{c}}_{u,n-2}, \quad U_{n-1} \rightarrow U_{n-1} - i_{n-1}\bar{\bar{R}}_{u,n-2} \end{aligned},$$

under which $E_{u,n-1}$ now becomes

$$g_{n-1}u_n + h_{n-1}u_{n-1} + \gamma_{n-1}v_{n-2} + j_{n-1}v_{n-1} + \alpha_{n-1}v_n = U_{n-1}.$$

Unknowns u_{n-1} and v_{n-2} are eliminated from this equation by using the transformations

$$\begin{aligned} j_{n-1} &\rightarrow j_{n-1} + \gamma_{n-1}\bar{\bar{a}}_{v,n-2} + h_{n-1}\bar{\bar{a}}_{u,n-1}, \\ \alpha_{n-1} &\rightarrow \alpha_{n-1} + \gamma_{n-1}\bar{\bar{b}}_{v,n-2} + h_{n-1}\bar{\bar{b}}_{u,n-1}, \\ \beta_{n-1} &= \quad\quad + \gamma_{n-1}\bar{\bar{c}}_{v,n-2} + h_{n-1}\bar{\bar{c}}_{u,n-1}, \\ U_{n-1} &\rightarrow U_{n-1} + \gamma_{n-1}\bar{\bar{R}}_{v,n-2} + h_{n-1}\bar{\bar{R}}_{u,n-1}. \end{aligned}$$

It only remains to eliminate v_{n-2} from $E_{v,n}$, using

$$\begin{aligned} d_n &\rightarrow d_n + e_n\bar{\bar{a}}_{v,n-2}, \quad & c_n &\rightarrow c_n + e_n\bar{\bar{b}}_{v,n-2}, \\ b_n &\rightarrow b_n + e_n\bar{\bar{c}}_{v,n-2}, \quad & V_n &\rightarrow V_n - e_n\bar{\bar{R}}_{v,n-2} \end{aligned}$$

and this step is repeated for $n = 5, 6, \ldots, N$. Employing the upper boundary conditions gives v_{N+1}, v_N and u_{N+1}, and then the modified $E_{u,N-1}$ implies that

$$v_{N-1} = \frac{U_{N-1}}{j_{N-1}}.$$

Using $(A6a)$ with $n = N$ gives $v_{N-2} = \phi_1(v_{N-1}, v_N, v_{N+1})$ and $(A6b)$ yields $u_{N-1} = \phi_2(v_{N-1}, v_N, v_{N+1})$. In this way it is straightforward to back substitute and find the solution.

APPENDIX B

In this appendix we summarise the algorithm used to solve the inhomogeneous equations given in (3.5). The method mimics the algorithm for the homogeneous case but with slight adaptation to allow for different boundary conditions. Additionally, the resulting system can be solved directly and does not require any iterations.

The boundary conditions at $y = 0$ (i.e. $u = v = v' = 0$) are used to initialise the technique; first it is noted that

$$u_2 = -\frac{g_2}{h_2} v_3 + \frac{U_2}{h_2}.$$

It is then possible to eliminate this quantity from the equation $E_{u,3}$, using the transformations,

$$U_3 \to U_3 - \frac{i_3 U_2}{h_2}, \qquad h_3 \to h_3 - \frac{i_3 g_2}{h_2}.$$

The next equations may now be solved to obtain the relationships

$$v_3 = \bar{\bar{a}}_{v,3} v_4 + \bar{\bar{b}}_{v,3} v_5 + \bar{\bar{c}}_{v,3} u_4 + \bar{\bar{\bar{R}}}_{v,3}, \tag{B1a}$$

$$u_3 = \bar{\bar{a}}_{u,3} v_4 + \bar{\bar{b}}_{u,3} v_5 + \bar{\bar{c}}_{u,3} u_4 + \bar{\bar{\bar{R}}}_{u,3}. \tag{B1b}$$

These functions are eliminated from the equations $E_{u,4}$ and $E_{v,4}$ by implementing the transformations

$$c_4 \to c_4 + d_4 \bar{\bar{a}}_{v,3}, \quad b_4 \to b_4 + d_4 \bar{\bar{b}}_{v,3}, \quad f_4 \to f_4 + d_4 \bar{\bar{c}}_{v,3}, \quad V_4 \to V_4 - d_4 \bar{\bar{\bar{R}}}_{v,3},$$

$$j_4 \to j_4 + i_4 \bar{\bar{a}}_{u,3}, \quad \alpha_4 = i_4 \bar{\bar{b}}_{u,3}, \quad h_4 \to h_4 + i_4 \bar{\bar{c}}_{u,3}, \quad U_4 \to U_4 - i_4 \bar{\bar{\bar{R}}}_{u,3}.$$

The current equations may now be solved to obtain expressions for v_4 and u_4 similar to those in (B1). This procedure can be generalised and represented as follows. Once expressions similar to $(B1a, b)$ have been derived for u_{n-1}, v_{n-1} and v_{n-2} then write

$$j_n \to j_n + i_n \bar{\bar{a}}_{v,n-1}, \qquad \alpha_n = i_n \bar{\bar{b}}_{v,n-1},$$
$$h_n \to h_n - i_n \bar{\bar{c}}_{v,n-1}, \qquad U_n \to U_n - i_n \bar{\bar{\bar{R}}}_{v,n-1}$$

and

$$d_n \to d_n + e_n \bar{\bar{a}}_{v,n-2}, \qquad c_n \to c_n + e_n \bar{\bar{b}}_{v,n-2},$$
$$\gamma_n = e_n \bar{\bar{c}}_{v,n-2}, \qquad V_n \to V_n - e_n \bar{\bar{\bar{R}}}_{v,n-2}$$

where γ_n is the coefficient of u_{n-1} in $E_{v,n}$. To eliminate v_{n-1} and u_{n-1} from $E_{v,n}$ the transformations are used

$$c_n \rightarrow c_n + d_n\bar{\bar{a}}_{v,n-1} + \gamma_n\bar{\bar{a}}_{u,n-1}, \qquad b_n \rightarrow b_n + d_n\bar{\bar{b}}_{v,n-1} + \gamma_n\bar{\bar{b}}_{u,n-1},$$

$$f_n \rightarrow f_n + d_n\bar{\bar{c}}_{v,n-1} + \gamma_n\bar{\bar{c}}_{u,n-1}, \qquad V_n \rightarrow V_n - d_n\bar{\bar{R}}_{v,n-1} - \gamma_n\bar{\bar{R}}_{u,n-1},$$

are used. The forms of the double over-barred terms may be generalised according to

$$\bar{\bar{a}}_{v,n} = \frac{-b_n + \frac{f_n\alpha_n}{h_n}}{\Gamma_n}, \qquad \bar{\bar{b}}_{v,n} = -\frac{a_n}{\Gamma_n}, \qquad \bar{\bar{c}}_{v,n} = \frac{f_n g_n}{\Gamma_n h_n},$$

$$\bar{\bar{R}}_{v,n} = \frac{V_n - \frac{f_n U_n}{h_n}}{\Gamma_n}, \qquad \bar{\bar{a}}_{u,n} = -\frac{\alpha_n}{h_n} - \frac{j_n\bar{\bar{a}}_{v,n}}{h_n}, \qquad \bar{\bar{b}}_{u,n} = -\frac{j_n\bar{\bar{b}}_{v,n}}{h_n},$$

$$\bar{\bar{c}}_{u,n} = -\frac{g_n}{h_n} - \frac{j_n\bar{\bar{c}}_{v,n}}{h_n}, \qquad \bar{\bar{R}}_{u,n} = \frac{U_n}{h_n} - \frac{j_n V_n}{h_n},$$

with $\Gamma_n = c_n - f_n j_n/h_n$.

This procedure is repeated until the upper limit of the solution space is reached (entirely analogous to the method given in Appendix A). It is then elementary to back substitute and deduce the solution.

In the solution of the small wavenumber equations (6.2) it was known from the results of Hall (1985) that the most dangerous mode for this system corresponds to eigenfunctions which are even in the co-ordinate $\hat{\tilde{\psi}}$. In order to solve (6.2) it was therefore convenient to only consider the domain $[0,\ \infty)$ and alter the boundary conditions at $\hat{\tilde{\psi}} = 0$ in order to ensure that an even-valued eigenfunction set was indeed derived. In the process of doing this it was important that the third derivative of a function was calculated accurately when the iteration process on the desired eigenvalues was applied. The discretisations discussed in Appendix A were found to be insufficiently precise for this purpose and therefore higher order discretisations were required. For example, the second derivative of a function at the origin was now written as

$$\begin{aligned}
\frac{d^2\phi}{dy^2} =& \frac{2\phi_1(h_1h_2h_3 + h_1h_2h_4 + h_1h_3h_4 + h_2h_3h_4 + h_2h_3h_5 + h_1h_4h_5 + h_2h_4h_5 + h_3h_4h_5)}{h_1h_2h_3h_4h_5} \\
&- \frac{2\phi_2(h_2h_3h_4 + h_2h_3h_5 + h_2h_4h_5 + h_3h_4h_5)}{h_1(h_2-h_1)(h_3-h_1)(h_4-h_1)(h_5-h_1)} \\
&+ \frac{2\phi_3(h_1h_3h_4 + h_1h_3h_5 + h_1h_4h_5 + h_3h_4h_5)}{(h_1-h_2)h_2(h_3-h_2)(h_4-h_2)(h_2-h_5)} \\
&+ \frac{2\phi_4(h_1h_2h_4 + h_1h_2h_5 + h_1h_4h_5 + h_2h_4h_5)}{(h_1-h_3)(h_2-h_3)h_3(h_4-h_3)(h_3-h_5)} \\
&+ \frac{2\phi_5(h_1h_2h_3 + h_1h_2h_5 + h_1h_3h_5 + h_2h_3h_5)}{(h_1-h_4)(h_2-h_4)(h_4-h_3)h_4(h_5-h_4)} \\
&+ \frac{2\phi_6(h_1h_2h_3 + h_1h_2h_4 + h_1h_3h_4 + h_2h_3h_4)}{(h_1-h_5)(h_2-h_5)(h_3-h_5)h_5(h_5-h_4)},
\end{aligned}$$

where $h_j = y_{j+1} - y_1$. Similar expressions were used for the third and fourth derivatives at the origin and neighbouring points but they are not included here for reasons of brevity. However details may be obtained upon application to either author.

References

Baskaran, V. & Bradshaw, P. 1988 Decay of spanwise inhomogeneities in a three–dimensional turbulent boundary layer over an infinite swept concave wall. *Experiments in Fluids* **6**, 487–492.

Bassom, A.P. 1992 Time dependent inviscid vortices in three–dimensional boundary layers. *Q. J. Mech. appl. Maths, in press.*

Bassom, A.P. & Blennerhassett, P.J. 1992 On the generation of mean flows by strongly nonlinear vortices in high Taylor number channel flows. *Applied Mathematics Preprint AM92/5, University of New South Wales..*

Bassom, A.P. & Hall, P. 1991 Vortex instabilities in three–dimensional boundary layers: The relationship between Görtler and Crossflow vortices. *J. Fluid Mech.* **232**, 647–680.

Bassom, A.P. & Seddougui, S.O. 1990 The onset of three–dimensionality and time–dependence in Görtler vortices: neutrally stable wavy modes. *J. Fluid Mech.* **220**, 661–672.

Dando, A.H. 1992 The inviscid compressible Görtler problem in 3D boundary layers. *Submitted to Theoret. Comput. Fluid Dyn..*

Denier, J.P. 1992 The development of fully nonlinear Taylor vortices. *IMA J. Appl. Maths, in press.*

Denier, J.P. & Hall, P. 1991 On the nonlinear development of the most unstable Görtler vortex mode. *ICASE Report No. 91-86, submitted to J. Fluid Mech..*

Denier, J.P., Hall, P. & Seddougui, S. 1991 On the receptivity problem for Görtler vortices: vortex motion induced by wall roughness. *Phil. Trans. Roy. Soc. Lond. A* **335**, 51–85.

Görtler, H. 1940 Uber eine dreidimensionale instabilität laminare Grenzschubten an Konkaven Wänden. *NACA TM 1357.*

Gregory, N., Stuart, J.T. & Walker, W.S. 1955 On the stability of three dimensional boundary layers with application to the flow due to a rotating disk. *Phil. Trans. R. Soc. Lond. A* **248**, 155–199.

Hall, P. 1982a Taylor–Görtler vortices in fully developed or boundary layer flows. *J. Fluid Mech.* **124**, 475–494.

Hall, P. 1982b On the nonlinear evolution of Görtler vortices in non–parallel boundary layers. *J. Inst. Maths Applics* **29**, 173–196.

Hall, P. 1983 The linear development of Görtler vortices in growing boundary layers. *J. Fluid Mech.* **130**, 41–58.

Hall, P. 1985 The Görtler vortex instability mechanism in three–dimensional boundary layers. *Proc. Roy. Soc. Lond. A* **399**, 135–152.

Hall, P. 1988 The nonlinear development of Görtler vortices in growing boundary layers. *J. Fluid Mech.* **193**, 247–266.

Hall, P. 1990 Görtler vortices in growing boundary layers: the leading edge receptivity problem, linear growth and the nonlinear breakdown stage. *Mathematika* **37**, 151–189.

Hall, P. & Lakin, W.D. 1988 The fully nonlinear development of Görtler vortices in growing boundary layers. *Proc. R. Soc. Lond. A* **415**, 421–444.

Hall, P. & Seddougui, S.O. 1989 On the onset of three-dimensionality and time-dependence in Görtler vortices. *J. Fluid Mech.* **204**, 405–420.

Hämmerlin, G. 1956 Zur Theorie der dreidimensionalen Instabilitat laminar Grenschichten. *Z. Angew. Math. Phys.* **1**, 156–167.

Malik, M.R., Chuang, S. & Hussaini, M.Y. 1982 Accurate numerical solution of the compressible linear stability equations. *Z. Angew. Math. Phys.* **33**, 189–201.

Peerhossaini, H. & Wesfreid, J.E. 1988a On the inner structure of streamwise Görtler rolls. *Int. J. Heat Fluid Flow* **9**, 12–18.

Peerhossaini, H. & Wesfreid, J.E. 1988b Experimental study of the Taylor–Görtler instability. In *Propagation in Systems Far from Equilibrium* (ed. J.E. Wesfreid, H.R. Brand, P. Manneville, G. Albinet & N. Boccara). Springer Series in Synergetics, vol. 41, pp. 399–412. Springer.

Seddougui, S.O. & Bassom, A.P. 1991 On the instability of Görtler vortices to nonlinear travelling waves. *IMA J. Appl. Maths* **46**, 269–296.

Smith, A.M.O. 1955 On the growth of Taylor–Görtler vortices along highly concave walls. *Q. Appl. Maths* **13**, 233–262.

Stuart, J.T. 1960 On the nonlinear mechanics of wave disturbances in stable and unstable parallel flows, Part 1. The basic behaviour in plane Poiseuille flow. *J. Fluid Mech.* **9**, 353–370.

Watson, J. 1960 On the nonlinear mechanics of wave disturbances in stable and unstable parallel flows, Part 2. The development of a solution for plane Poiseuille and plane Couette flow. *J. Fluid Mech.* **9**, 371–389.

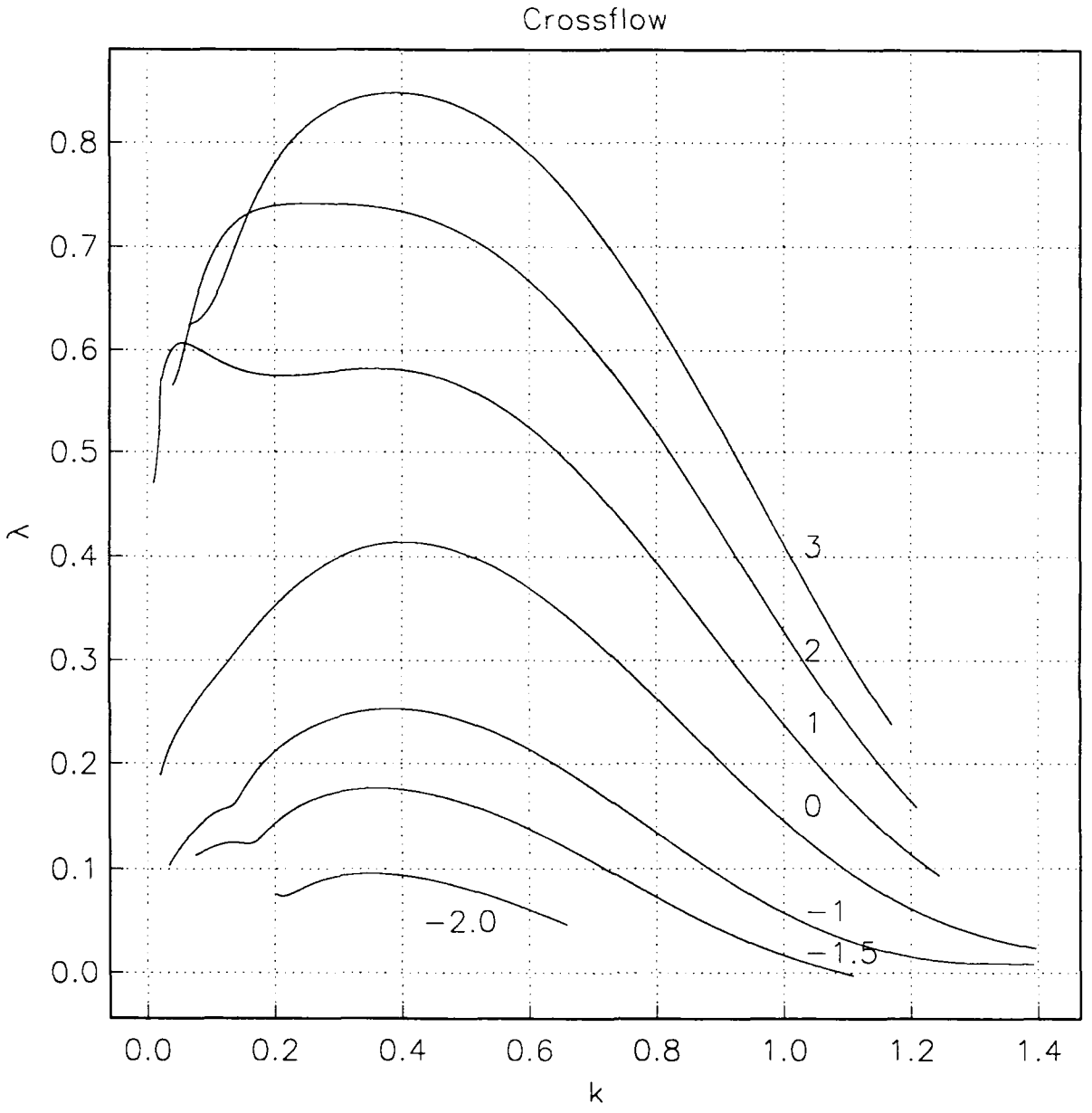

Figure 1. The crossflow parameter λ needed to ensure the neutral stability of vortices of various frequencies. $\Omega_0 = 3.0, 2.0, 1.0, 0, -1, -1.5, -2$.

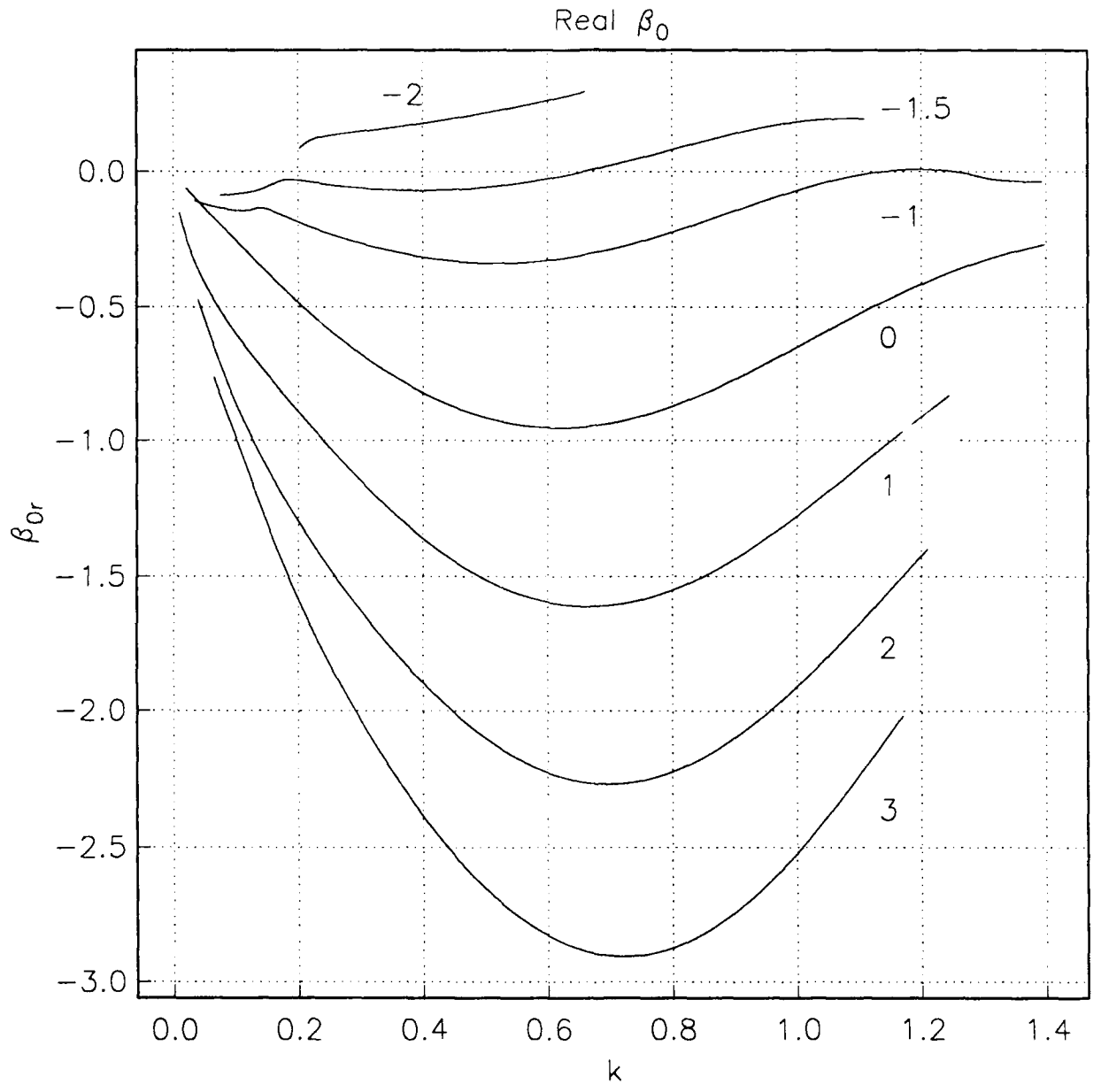

Figure 2. The streamwise variation parameter β_0 of neutrally stable vortices of various frequencies. $\Omega_0 = 3.0, 2.0, 1.0, 0, -1, -1.5, -2$.

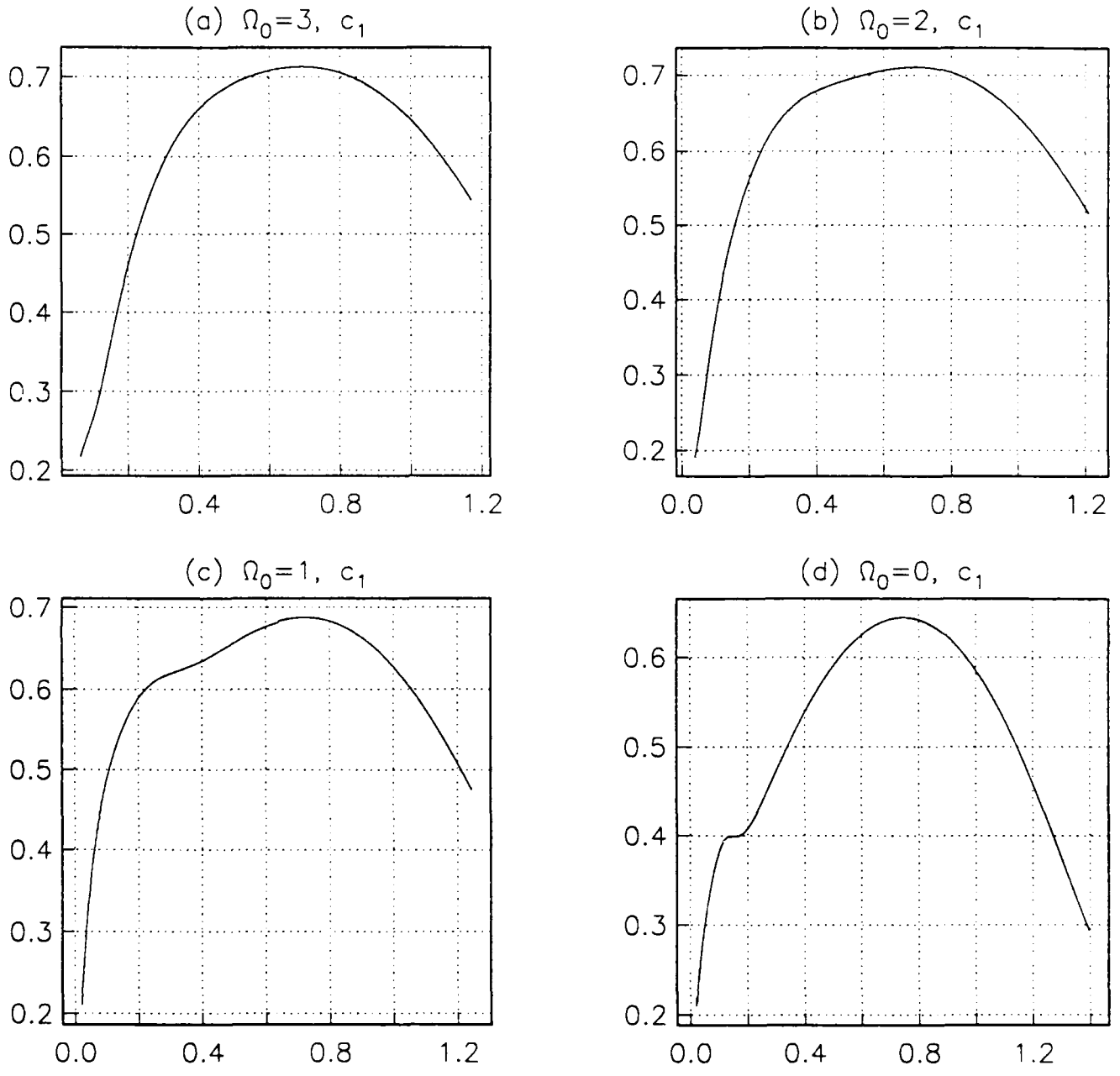

Figure 3. The coefficient c_1 of amplitude equation (3.9) as a function of the vortex wavenumber k for $\Omega_0 = (a)$ 3, (b) 2, (c) 1, (d) 0, (e) -1, (f) -1.5 and (g) -2.

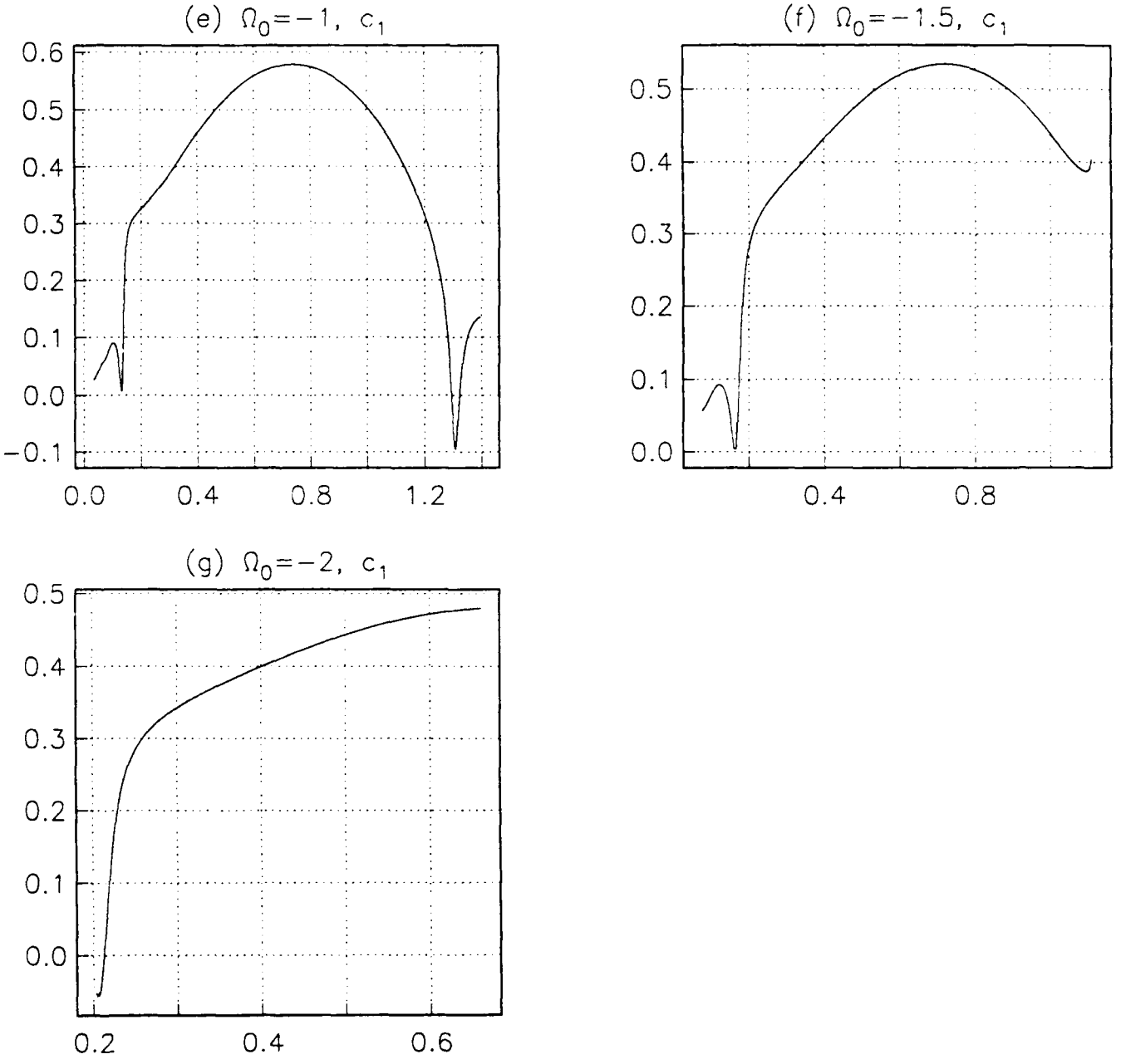

Figure 3. The coefficient c_1 of amplitude equation (3.9) as a function of the vortex wavenumber k for $\Omega_0 = (a)$ 3, (b) 2, (c) 1, (d) 0, (e) -1, (f) -1.5 and (g) -2.

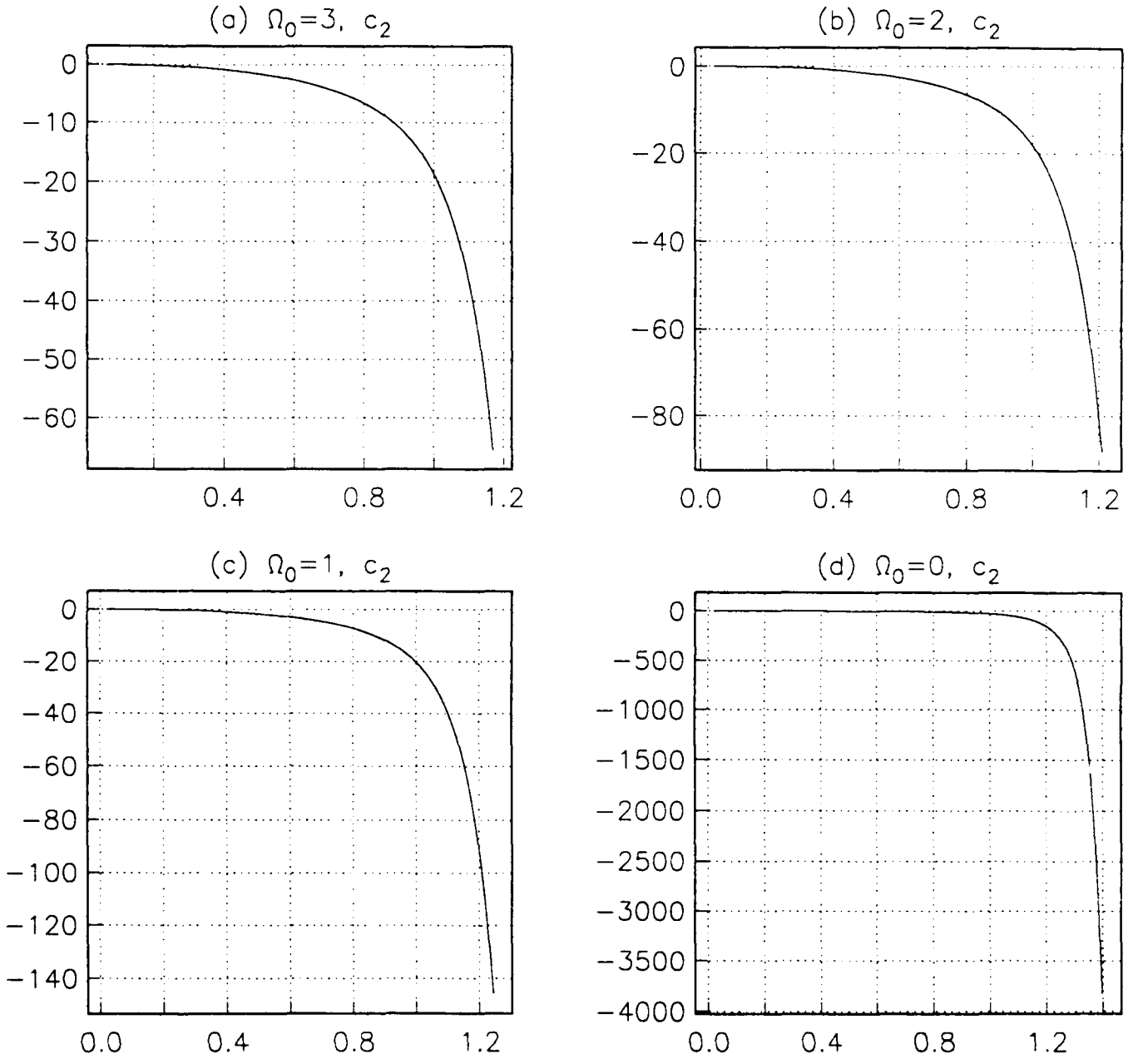

Figure 4. The coefficient c_2 of amplitude equation (3.9) as a function of the vortex wavenumber k for $\Omega_0 = (a)\ 3, (b)\ 2, (c)\ 1, (d)\ 0, (e)\ -1, (f)\ -1.5$ and $(g)\ -2$.

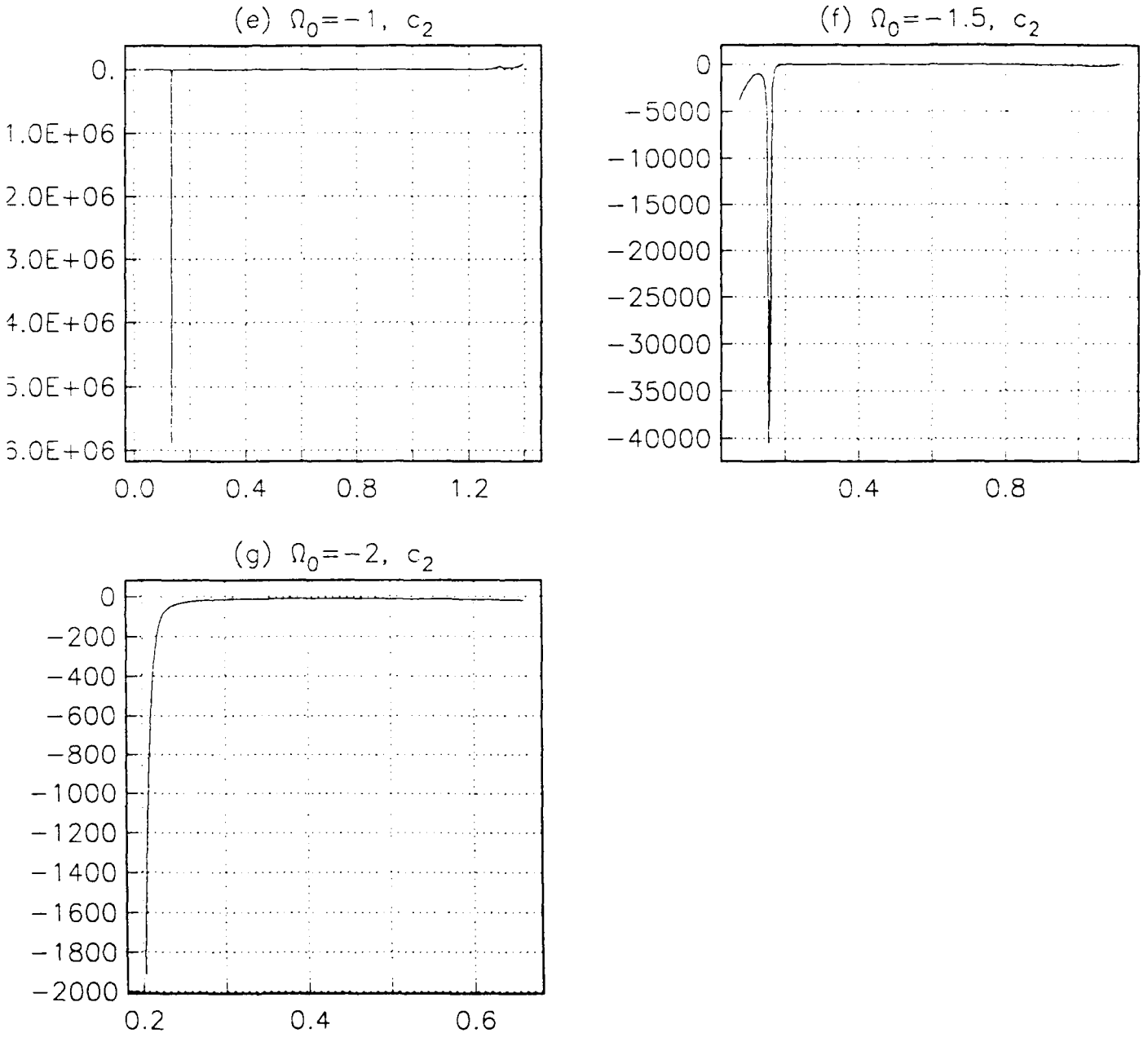

Figure 4. The coefficient c_2 of amplitude equation (3.9) as a function of the vortex wavenumber k for $\Omega_0 = (a)$ 3, (b) 2, (c) 1, (d) 0, (e) -1, (f) -1.5 and (g) -2.

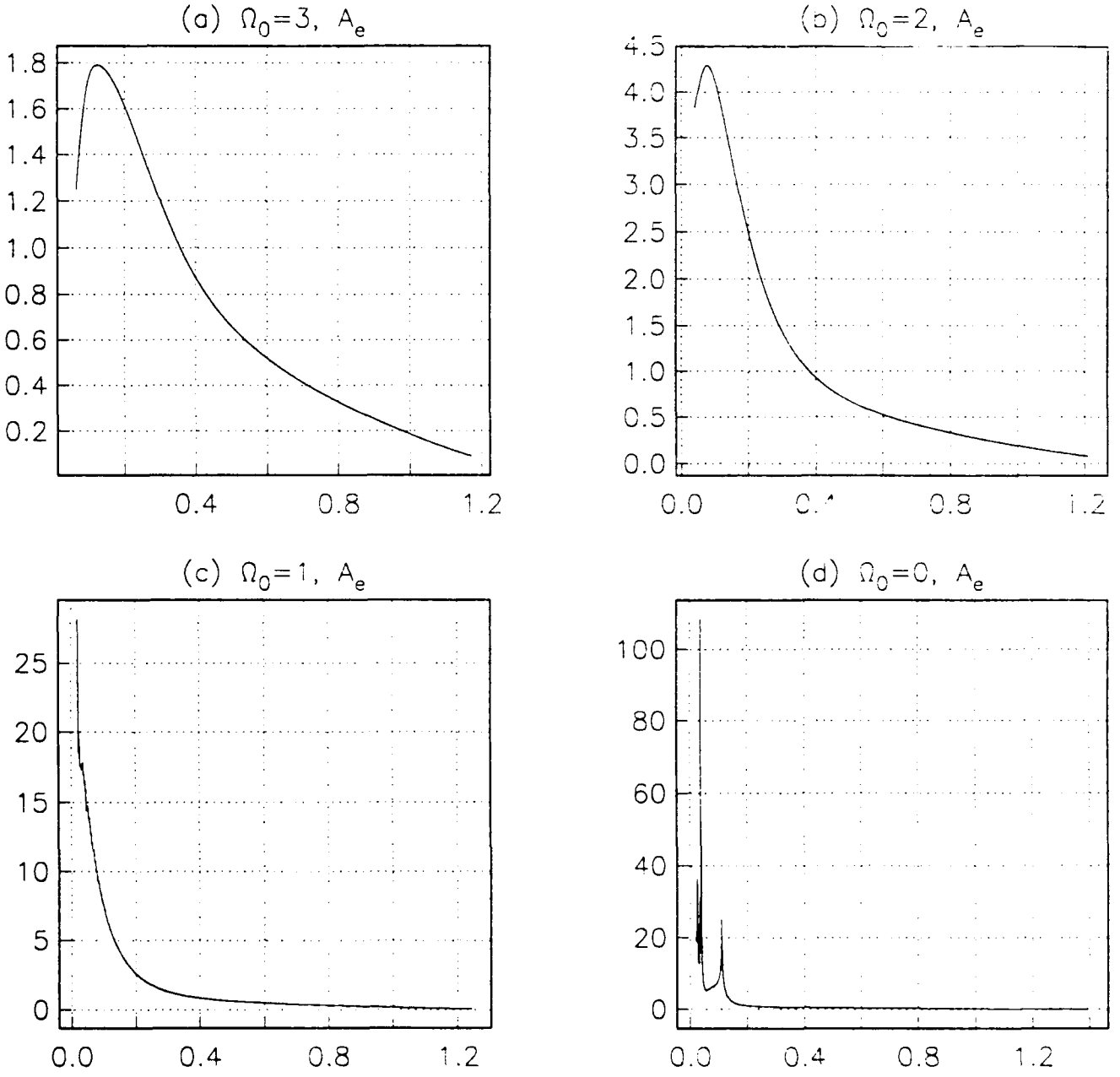

Figure 5. The equilibrium amplitude $\Omega_2^{-\frac{1}{2}}|A_e|$ (defined by (5.1)) as a function of the vortex wavenumber k for $\Omega_0 = (a)$ 3, (b) 2, (c) 1, (d) 0, (e) -1, (f) -1.5 and (g) -2.

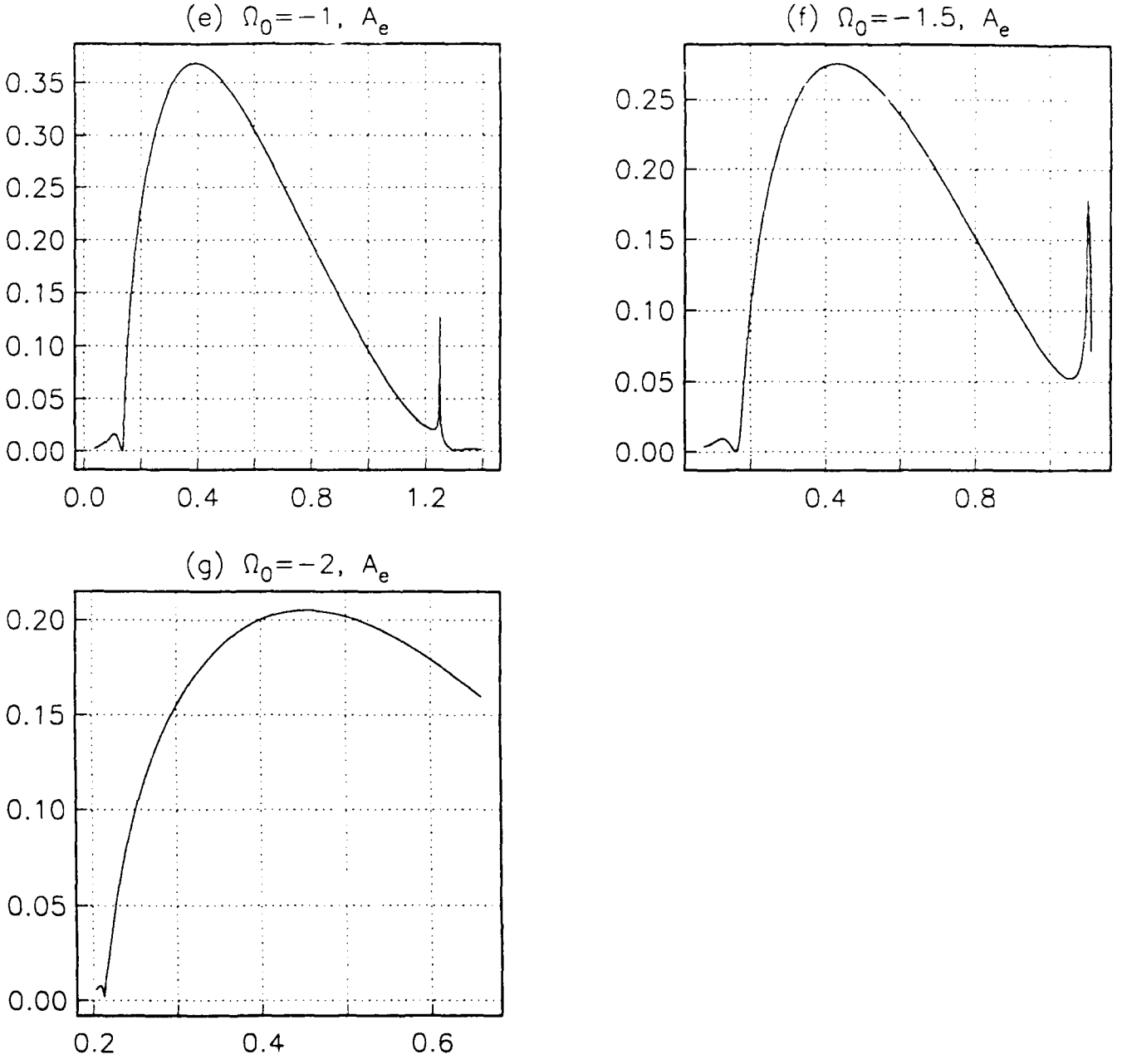

Figure 5. The equilibrium amplitude $\Omega_2^{-\frac{1}{2}}|A_e|$ (defined by (5.1)) as a function of the vortex wavenumber k for $\Omega_0 = (a)$ 3, (b) 2, (c) 1, (d) 0, (e) -1, (f) -1.5 and (g) -2.

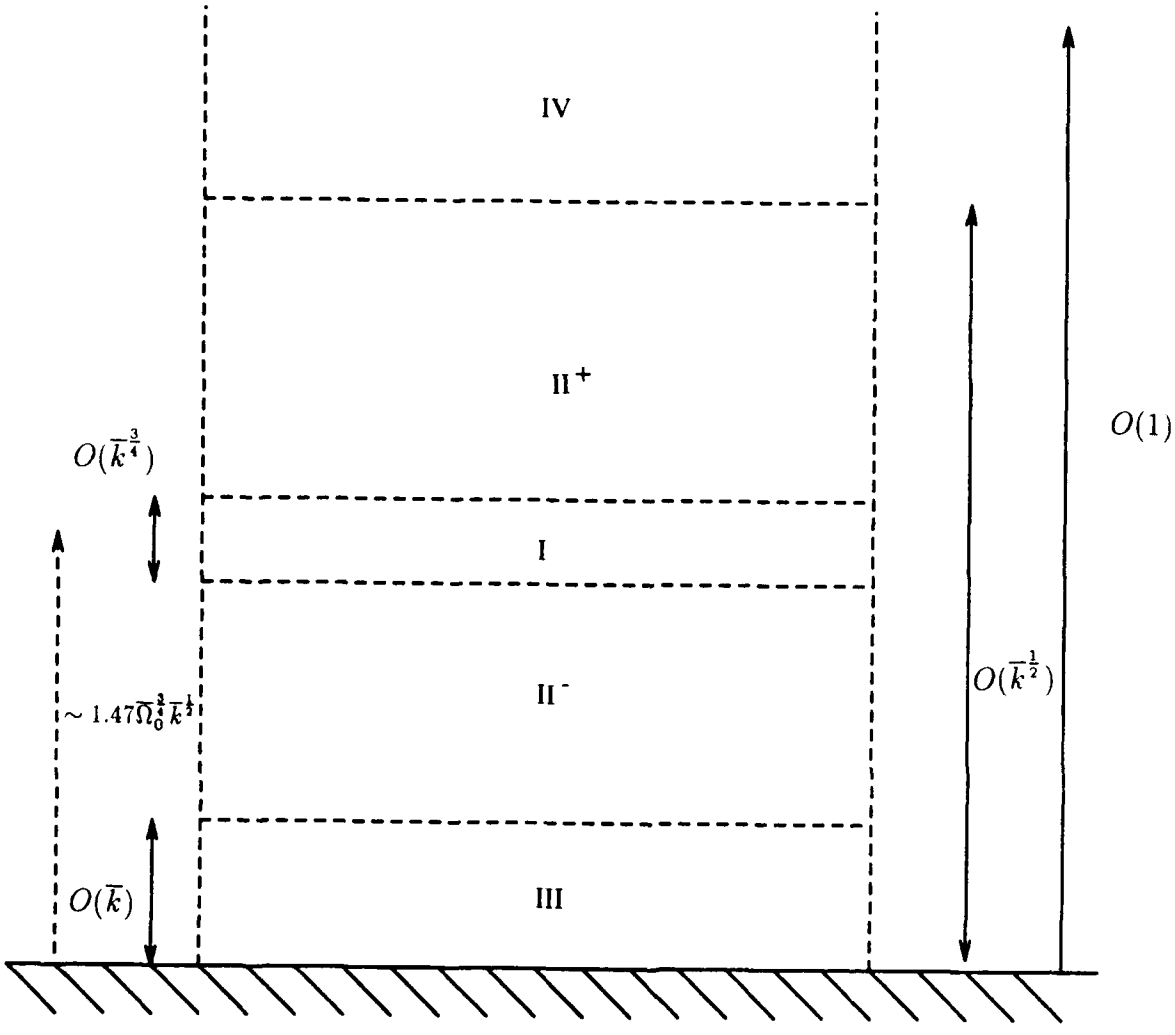

Figure 6. Schematic diagram of the asymptotic structure of the solution of homogeneous system (3.3) for the case of small vortex wavenumber $k \ll 1$. The solution configuration divides into four distinct zones: Zone I is a thin region of depth $O(k^{\frac{3}{4}})$ at a distance $\sim 1.47\Omega_0^{\frac{3}{8}} k^{\frac{1}{2}}$ from the wall. This zone is embedded within II, a region of thickness $O(k^{\frac{1}{2}})$. The structure has an additional viscous layer at the wall, zone III, which enables the boundary conditions there to be met. Finally, a region IV of depth $O(1)$ facilitates the exponential decay of the disturbance solutions far from the wall.

REPORT DOCUMENTATION PAGE

Form Approved
OMB No 0704-0188

1. AGENCY USE ONLY (Leave blank)	2. REPORT DATE	3. REPORT TYPE AND DATES COVERED
	April 1992	Contractor Report

4. TITLE AND SUBTITLE
ON THE STABILITY OF NONLINEAR VISCOUS VORTICES IN THREE-DIMENSIONAL BOUNDARY LAYERS

5. FUNDING NUMBERS
C NAS1-18605
WU 505-90-52-01

6. AUTHOR(S)
Andrew P. Bassom
S.R. Otto

7. PERFORMING ORGANIZATION NAME(S) AND ADDRESS(ES)
Institute for Computer Applications in Science and Engineering
Mail Stop 132C, NASA Langley Research Center
Hampton, VA 23665-5225

8. PERFORMING ORGANIZATION REPORT NUMBER
ICASE Report No. 92-15

9. SPONSORING/MONITORING AGENCY NAME(S) AND ADDRESS(ES)
National Aeronautics and Space Administration
Langley Research Center
Hampton, VA 23665-5225

10. SPONSORING/MONITORING AGENCY REPORT NUMBER
NASA CR-189637
ICASE Report No. 92-15

11. SUPPLEMENTARY NOTES
Langley Technical Monitor: Michael F. Card
Final Report
Submitted to Journal of Fluid Mechanics

12a. DISTRIBUTION/AVAILABILITY STATEMENT
Unclassified - Unlimited

Subject Category 34

12b. DISTRIBUTION CODE

13. ABSTRACT (Maximum 200 words)

Recently it has been demonstrated that three-dimensionality can play an important role in dictating the stability properties of any Görtler vortices which a particular boundary layer may support. According to a linearised theory vortices within a high Görtler number flow can take one of two possible forms within a two-dimensional flow supplemented by a small crossflow of size $O(R_e^{-1/2}G^{3/5})$ where R_e is the Reynolds number of the flow and G the Görtler number. Bassom & Hall (1991) showed that these forms are characterised by O(1) wavenumber inviscid disturbances and larger, $O(G^{1/5})$, wavenumber modes which are trapped within a thin layer adjacent to the bounding surface. Here we concentrate on the latter, essentially viscous vortices and describe their weakly nonlinear stability properties in the presence of crossflow. It is shown conclusively that the effect of crossflow is to stabilise the nonlinear disturbances and the calculations herein allow stable, finite amplitude perturbations to be found. Predictions are made concerning the likelihood of observing some of these viscous modes within a practical setting and asymptotic work permits discussion of the stability properties of modes with wavenumbers which are small relative to the implied $O(G^{1/5})$ scaling.

14. SUBJECT TERMS	15. NUMBER OF PAGES
crossflow, nonlinear, 'viscous vortices'	49
	16. PRICE CODE: A03

17. SECURITY CLASSIFICATION OF REPORT	18. SECURITY CLASSIFICATION OF THIS PAGE	19. SECURITY CLASSIFICATION OF ABSTRACT	20. LIMITATION OF ABSTRACT
Unclassified	Unclassified		